JPC 431

Report Number
TM-67-1

Analytical Studies of the Interior Ballistics of Spinning Rocket Motors - A Literature Survey

by

D. J. Norton

B. W. Farquhar

J. D. Hoffman

Technical Memorandum

Contract No. DA-01-021-AMC-15257(Z)

January 1967

JET PROPULSION CENTER
PURDUE UNIVERSITY

SCHOOL OF MECHANICAL ENGINEERING
LAFAYETTE, INDIANA

Citation Format: Full Citation (1F)

Accession Number:
AD0814933
Citation Status:
Active
Citation Classification:
Unclassified
Fields and Groups:
200400 - Fluid Mechanics
210802 - Solid Propellant Rocket Engines
Corporate Author:
PURDUE UNIV LAFAYETTE IN JET PROPULSION CENTER
Unclassified Title:
(U) ANALYTICAL STUDIES OF THE INTERIOR BALLISTICS OF SPINNING ROCKET MOTORS - A LITERATURE SURVEY.
Title Classification:
Unclassified
Descriptive Note:
Technical memo.,
Personal Author(s):
Norton, D J
Farquhar, B W
Hoffman, J D
Report Date:
Jan 1967
Media Count:
107 Page(s)
Cost:
$14.60
Contract Number:
DA-01-021-AMC-15257(Z)
Report Number(s):
TM-67-1
JPC-431
Report Classification:
Unclassified
Descriptors:
(U) *SOLID PROPELLANT ROCKET ENGINES, *ROCKET ENGINES, NOZZLE GAS FLOW, INTERIOR BALLISTICS, VORTICES, STATE OF THE ART, REPORTS, COMPRESSIVE PROPERTIES, ACCELERATION, NAVIER STOKES EQUATIONS, SPINNING(MOTION), VISCOSITY, LAMINAR BOUNDARY LAYER, STABILITY, PHYSICAL PROPERTIES, ROTATION, BURNING RATE, BOUNDARY LAYER, SECONDARY FLOW, FLOW FIELDS, COMBUSTION CHAMBERS, ROCKET NOZZLES
Identifier Classification:
Unclassified

Abstract:

(U) This survey reviews the analytical literature pertinent to contained rotating flows. A related survey of the experimental literature is reported in TM 67-2. The main emphasis in this report is placed upon possible applications to the study of the fluid mechanics in rotating rocket motors. Since this area is only now receiving analytical attention it was necessary to draw heavily upon the classical analytical studies of vortex tubes and swirling flows in cylinders and converging nozzles. A great deal of the classical fluid mechanics in this area is incompressible in nature, therefore, must be considered qualitative in relation to actual rocket motors. Conditions existing in the nozzle and chamber are reviewed. In addition other topics such as, end wall interactions and boundary layers are reported upon. The analytical models for the determination of the effects of acceleration on the burning rate of solid propellants which have been reported in two recent papers are reviewed. (Author)

Abstract Classification:

Unclassified

Distribution Limitation(s):

01 - APPROVED FOR PUBLIC RELEASE

Source Code:

191100

Document Location:

DTIC AND NTIS

Change Authority:

ST-A USAMC LTR, 13 MAR 68

PURDUE UNIVERSITY

AND

PURDUE RESEARCH FOUNDATION
Lafayette, Indiana

Report No. TM-67-1

ANALYTICAL STUDIES OF THE INTERIOR BALLISTICS OF SPINNING ROCKET MOTORS - A LITERATURE SURVEY

by

D. J. Norton, B. W. Farquhar, J. D. Hoffman

Technical Memorandum

Contract No. DA-01-021-AMC-15257(Z)

United States Army Missile Command

Redstone Arsenal, Alabama

Jet Propulsion Center
Purdue University

January 1967

ACKNOWLEDGEMENTS

This review of the analytical literature pertaining to contained rotating flows was supported by the United States Army Missile Command, Redstone Arsenal, Alabama, under Contract Number DA-021-AMC-15257(Z). Mr. W. D. Guthrie was the technical monitor for the U. S. Army Missile Command.

Dr. Mel L'Ecuyer of the Jet Propulsion Center is gratefully acknowledged for his suggestions during the writing and preparation of this report. Dr. M. J. Zucrow, Professor Emeritus, and Dr. B. A. Reese, Director of the Jet Propulsion Center, are also recognized for their contributions to, and supervision of this research project.

TABLE OF CONTENTS

TABLE OF CONTENTS (cont'd.)

LIST OF ILLUSTRATIONS

ABSTRACT

This survey reveiws the analytical literature pertinent to contained rotating flows. A related survey of the experimental literature is reported in TM 67-2. The main emphasis in this report is placed upon possible applications to the study of the fluid mechanics in rotating rocket motors. Since this area is only now receiving analytical attention it was necessary to draw heavily upon the classical analytical studies of vortex tubes and swirling flows in cylinders and converging nozzles. A great deal of the classical fluid mechanics in this area is incompressible in nature, therefore, must be considered qualitative in relation to actual rocket motors. Conditions existing in the nozzle and chamber are reviewed. In addition other topics such as, end wall interactions and boundary layers are reported upon. The analytical models for the determination of the effects of acceleration on the burning rate of solid propellants which have been reported in two recent papers are reveiwed.

1.0 INTRODUCTION

The material presented in this literature survey will consist of analytical attempts to describe the difficult problem of contained rotating flows. The main emphasis is placed upon the theory of vortex flows in rocket motors. As yet, there is not a great deal of analytical work specifically oriented towards vortex flows in rocket motors. However, there has been a great deal of interest in vortex flows in general over the years. Therefore, many of the articles reviewed must be considered supplementary in nature, yet most of the fundamental points pertinent to rocket vortices are covered.

The discovery of the Ranque-Hilsch vortex tube stimulated a renewal of interest in vortex flow theory. Many of the theories developed to understand this device have applicability to the conditions existing in the chamber of rotating solid propellant rocket motors.

The study of rotating disks provides an insight into the problem of the interaction of the end walls with chamber flow field. The long familiar bathtub vortex in which a vortex is generated and flows toward a sink prompted early interest in vortex flow in nozzles. Much of the early work was for an incompressible perfect fluid. It was noted that the flow rate in such a nozzle was less than that for a non-rotating nozzle. Later, the addition of compressibility effects made it necessary to consider a void region near the axis, since the potential vortex possess the tendency toward infinite centerline velocities. The addition of viscous effects

further complicated the theory in that a solid body type vortex is necessarily established at the center line so that the free boundary conditions at the axis are satisfied.

Recently, the possibility of the existence of regions of reversed axial flow has been introduced to explain some apparently anomolous experimental results. Flow reversal has been attributed to both viscous effects such as end wall boundary layer interactions with the primary flow field, and, dynamic effects wherein finite transitions occur between two conjugate flows. The latter of these is referred to as vortex breakdown and is usually associated with a stagnation region on the axis with locally reversed flow.

The literature survey also includes two published theories of burning rate augmentation in spinning rocket motors. The fact that the propellant is burning differently from the non-rotating case is important in establishing the initial conditions for any detailed study of the flow.

Finally, two articles are presented in which the entire rocket motor, the chamber, the end walls, and the nozzle are considered to determine the ability of the vortex to effect the overall performance of the motor.

2.0 COMPRESSIBLE VORTEX FLOWS IN NOZZLES

2.1 Introduction

The flow of a vortex in a nozzle has been studied for a great many years. Historically the first theories were presented for the inviscid, irrotational flow of liquids. It was apparent from these calculations that the mass flow rate in a nozzle in which the fluid was rotating was not as great as the flow rate in a non-rotating case with similar chamber conditions. The formation of an air core along the axis of the liquid also served to reduce the mass flow rate. Later when compressible flow theory for gases was used an analogous situation developed in which the mass flux at the throat was reduced due to the rotating component. Similiar to the incompressible case a void region near the axis was predicted since the irrotational vortex predicts infinite tangential velocities at the center line. However, conservation of energy dictates that when the tangential velocity reaches the maximum isentropic speed further expansion is impossible since the pressure is zero.

Recently, in connection with end-burning rocket motors, the flow of a rotational vortex has been studied. These studies indicate a similiar decrease in the expected mass flow rate for given chamber conditions.

2.2 Irrotational Vortices

2.2.1 Theory of Binnie and Hooker

In a paper in 1937, Binnie and Hooker (1) discuss the radial and spiral flow of a compressible fluid in which a velocity potential is assumed to be definable.

$$\phi = A_\theta + B\, f(r) \tag{2.1}$$

Since a velocity potential is assumed, the flow field must be considered to be irrotational and homentropic. Therefore, the proper expressions for the tangential velocity and radial velocity are given by,

$$V = c/r = \frac{\partial \phi}{\partial \theta}\ ; \qquad u = \frac{\partial \phi}{\partial r} \tag{2.2}$$

It was shown that for radial flow of a swirling gas, the radial velocity must be less than in the case of no swirl. In addition, the radial velocity does not reach the sonic condition until the minimum cross sectional area is reached where the combined velocity of the gas is greater than the sonic velocity. The minimum area corresponds to the point where the area must begin increasing if the velocities are to continue increasing.

2.2.2 Theory of Binnie

In 1949, Binnie (2) again reported on the inviscid, adiabatic flow in an axisymmetric nozzle. In addition to other choking phenomena, the flow of a spiraling gas in a nozzle was discussed. As in previous work,

the tangential velocity was assumed to be given by,

$$V = c/r \tag{2.3}$$

so that the flow was irrotational. It was also assumed that the radial velocity was everywhere small so that it could be neglected.

Employing the Euler equations for axisymmetric, inviscid flow and neglecting radial velocities, Binnie derived the equation for mass flow in the nozzle.

$$\dot{m} = \int_{r_o}^{r_w} w\rho_o \left[1 - \frac{\gamma-1}{2}\left(\frac{w^2 + c^2/r^2}{a_o^2}\right)\right]^{1/\gamma-1} 2\pi r dr \tag{2.4}$$

where r_o = the radius of the inner void region

r_w = the radius of the nozzle wall

a_o = the stagnation accoustic speed

For analytical convenience, Binnie chose $\gamma = 2.0$ to study the character of the equations at the throat condition. Although not stated, it was assumed that the axial velocity was a constant at every cross section in the nozzle. Therefore, he was able to integrate the expression for mass flow rate. Then by differentiating that result with respect to the axial dimension and setting the result equal to zero, the conditions at the "throat" were found. It was shown that when $c = o$, the equation for the axial velocity reduces to the local speed of sound as in the case for one-dimensional flow. Binnie further illustrated that when $c \neq o$, the axial velocity must be some value less than the local speed of sound. This value of axial velocity was related to the value of the parameter, which

is the angular momentum of a streamline.

Binnie presents figures for the reduced axial velocity in the throat as a function of the ratio of the nozzle to void region radii and the angular momentum of a streamline. The figures were presented for $\gamma = 2$ and $\gamma = 1.4$.

In conclusion, this analysis was presented for an inviscid, irrotational, adiabatic flow in which radial velocities were neglected and axial velocities were assumed uniform over each cross section.

2.2.3 Theory of Mager

In 1961, Mager (3) made further contributions to the theory of swirling flow in a nozzle. As in the earlier work by Binnie, Mager assumed an irrotational, inviscid, adiabatic flow in which radial velocities are neglected and the axial velocity is assumed uniform in the radial direction. A schematic of the physical model is presented in Figure (1).

In his work, Mager assumed a velocity potential function of the following form:

$$\phi = [R_{(z)}\ W_{(z)}]\theta + \int W_{(z)} dz \qquad (2.4)$$

so that

$$u = \phi_r = 0; \qquad W = (RW)_z \theta + w; \qquad v = \frac{1}{r}\theta_\theta \ , \qquad (2.5)$$

and the total velocity is then given by

$$q^2 = (c^2/r^2 + w^2) \ . \qquad (2.6)$$

The mass flow rate through the nozzle is specified in the same manner as that determined by Binnie

$$\dot{m} = \int_{r_o}^{r} w\rho_o \left[1 - \frac{\gamma-1}{2a^2}\left(c^2/r^2 + w^2\right)\right]^{1/\gamma-1} 2\pi r dr = K_2 \qquad (2.7)$$

since,

$$V = c/r \ . \qquad (2.3)$$

It can be seen that as r approaches zero, the tangential velocity tends to infinity. However, the velocity of the gas is physically limited to the maximum isentropic velocity corresponding to zero temperature. Thus, an expression can be derived for the radius of the void region

$$r_o^2 = \left| \frac{\frac{\gamma-1}{2} c^2}{a_o^2 - \frac{\gamma-1}{2} w^2} \right| \ . \qquad (2.8)$$

The equation for mass flow can then be integrated for the selected values of γ which can be expressed in the following form.

$$\gamma = \frac{n+1}{n-1} \qquad (2.9)$$

Expressions for mass flow rate and specific impulse were then derived as a function of the parameter

$$\alpha = (c/R_{a_o}) \sqrt{\frac{\gamma-1}{2}} \ . \qquad (2.10)$$

Charts were presented illustrating the effect of the value of α at the "throat" upon the mass flow and thrust as compared to one-dimensional

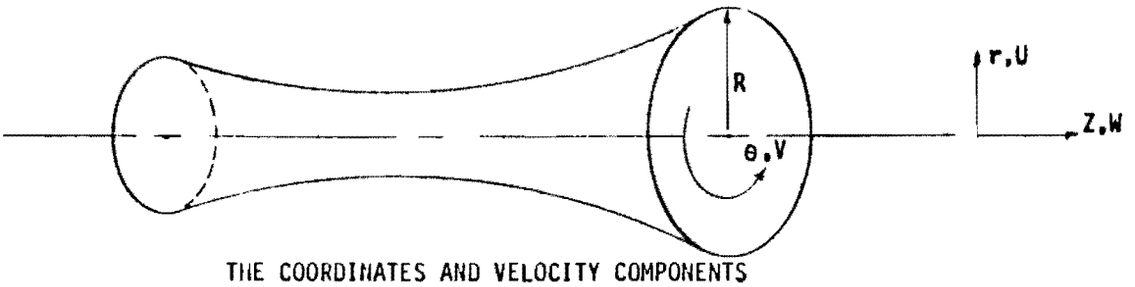

THE COORDINATES AND VELOCITY COMPONENTS
IN SWIRLING NOZZLE FLOW

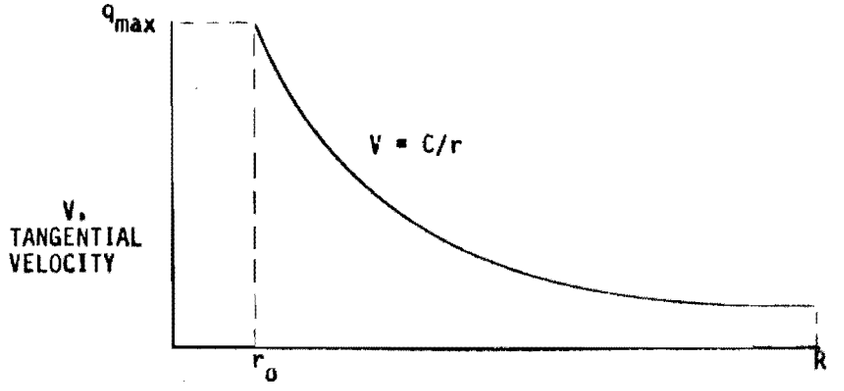

THE TANGENTIAL VELOCITY DISTRIBUTION FOR
THE IRROTATIONAL VORTEX

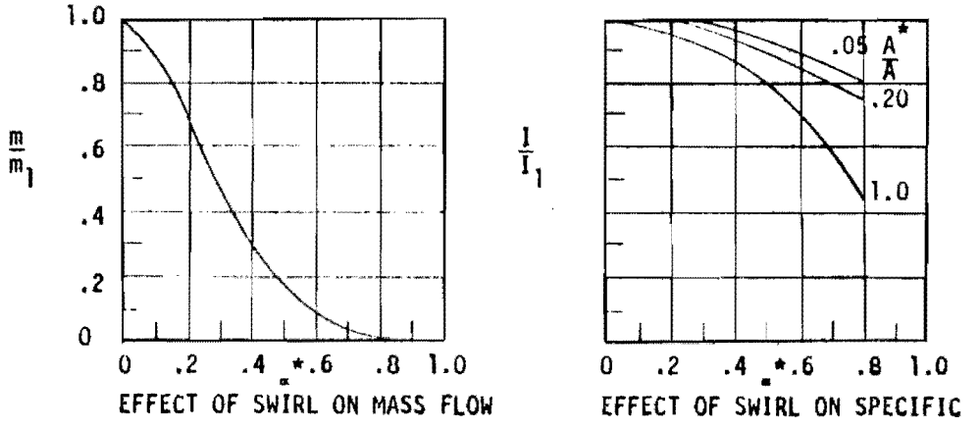

EFFECT OF SWIRL ON MASS FLOW

EFFECT OF SWIRL ON SPECIFIC
IMPULSE

FIGURE 1 THE MODEL AND SOME THEORETICAL RESULTS OF MAGER(3).
(Taken from reference (3) , Mager)

flow. It was shown that the greater the contraction ratio of the nozzle, the greater the reduction of the mass flow and specific impulse (Figure 1).

2.3 Rotational Vortices

2.3.1 Theory of Crocco and Vaszonyi

It was shown by Crocco and Vaszonyi (4,5,6), that when gradients exist in either the stagnation temperature or the stagnation pressure, the flow of the fluid is in general rotational. The generalized unsteady Crocco-Vaszonyi equation states

$$T\nabla S + \bar{q} \times \nabla \times \bar{q} = \nabla H_o + \frac{\partial \bar{q}}{\partial t} \tag{2.11}$$

and, for steady state,

$$\bar{q} \times \nabla \times \bar{q} = \bar{q} \times \bar{\omega} = \nabla H_o - T\nabla S \tag{2.12}$$

There are three conditions under which $\bar{q} \times \bar{\omega} = 0$. First,

$$\bar{q} = 0 \text{ which is a trivial case.} \tag{2.13}$$

Second,

$\bar{q} \times \bar{q} = \bar{\omega} = 0$ which is the case of an irrotational flow.

Third,

$\bar{q} \parallel \bar{\omega}$ - which is a special case of rotational vortex motion in which the vortex lines are everywhere parallel to the streamlines. This type of motion is called Beltrami Helical motion and can be derived from a uniformly translated, two-dimensional vortex in a constant area section.

Thus, in general, for the flow of a gas which has gradients in the stagnation properties,

$$\nabla s = cp \nabla \ln \left| \frac{T_0}{P_0^{\frac{\gamma-1}{\gamma}}} \right| \tag{2.14}$$

Thus, the entropy is not constant in the direction normal to the streamlines, and the flow is rotational. Substituting eqn. 2.14 into eqn. 2.12 gives the following result,

$$\bar{q} \times \bar{\omega} = cp \nabla T_0 - T \nabla \ln \left(\frac{T_0}{P_0^{\frac{\gamma-1}{\gamma}}}\right) \neq 0 , \tag{2.15}$$

except when, T_0 and P_0 are constants. Therefore if gradients exist in either T_0, or P_0 the flow field must be considered rotational.

A further consequence of variations of stagnation properties is that the well known law of Kelvin in which the circulation for a barotropic fluid is constant for all time, is no longer applicable. A barotropic flow exists when there is a unique relationship between the pressure and density. The two most important examples are incompressible flow and isentropic flow. In a flow which has variations in the stagnation properties, there no longer exists a unique relationship between the pressure and density normal to the streamlines. However, along a streamline, the flow may still be isentropic.

Thus, the circulation Γ, which is given by the expression

$$\Gamma = \oint \bar{V} \cdot d\bar{l} \tag{2.16}$$

is no longer a constant in each plane.

2.3.2 Theory of Bastress

The first study of the flow of a rotational vortex in a nozzle was presented by Bastress (7) in 1965. This analysis was followed by several others which are essentially similar. However, each exhibits certain refinements. Since the stagnation properties are in general not constant normal to the streamlines, numerical calculations associated with these analyses rely upon average properties within stream shells. A stream shell is defined as an annulus through which a given amount of mass, energy and momentum are flowing and across which the stagnation properties are averaged, as illustrated in Fig. 2.

The following set of assumptions is common to all the analyses presented in this section.

1. Steady flow
2. Inviscid flow
3. Adiabatic flow
4. Perfect gases
5. Negligible radial velocities

It assumed either directly or by implication that a solid body vortex persists at every cross section of the nozzle. In addition, all analyses are basically one-dimensional in that only radial variations of the properties of the flow are allowed. However, both tangential and axial velocities are considered. A schematic of the physical model is given in Fig. 2.

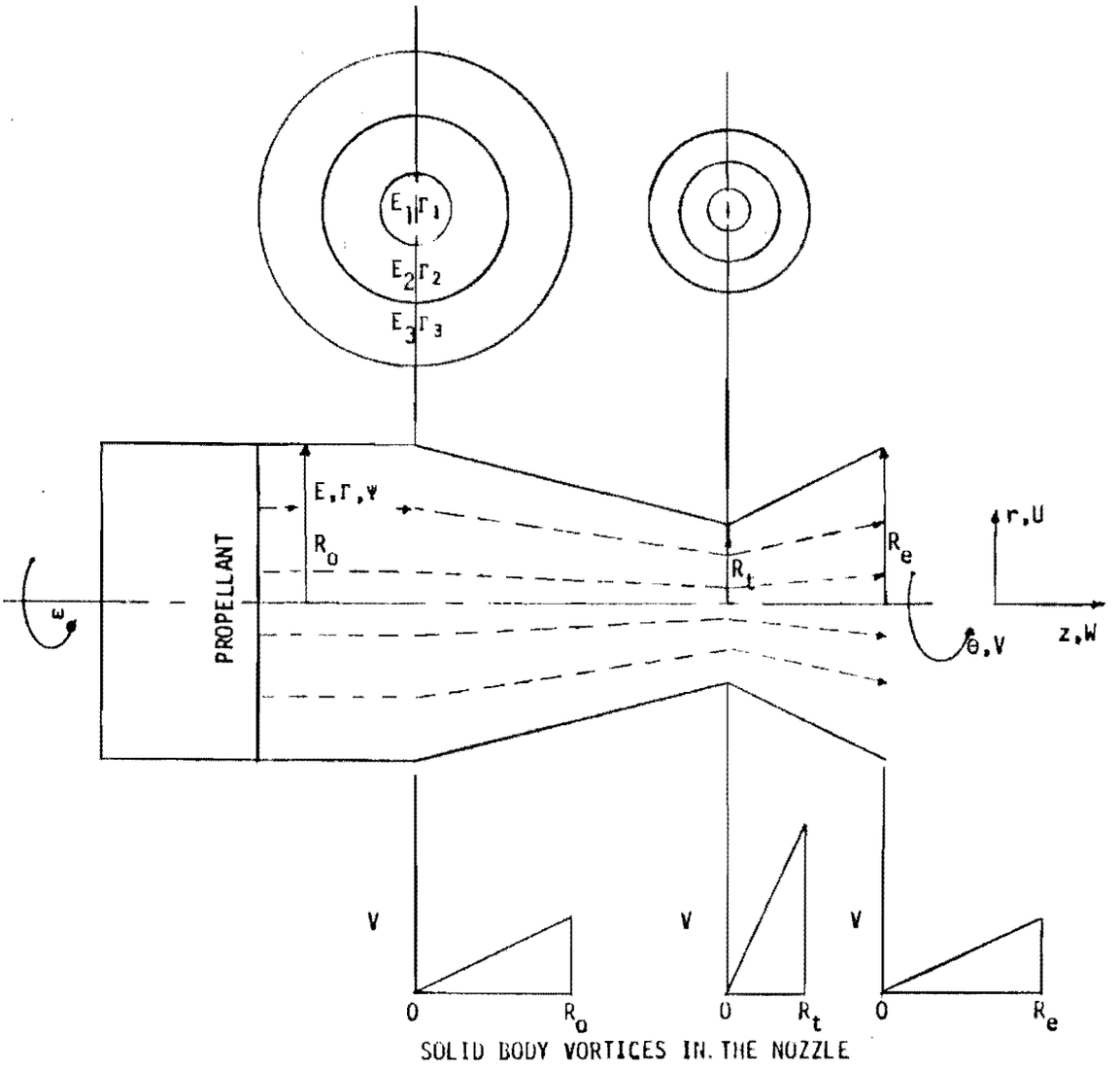

FIGURE 2 THE MODEL FOR THE ROTATIONAL, COMPRESSIBLE, VORTEX FLOWS IN NOZZLES

In the work by Bastress, the following equations are considered.

State $$P = \rho R t \tag{2.17}$$

Energy $$c_p T_o = c_p t + \frac{w^2 + v^2}{2} \tag{2.18}$$

Angular momentum $$\omega_o r_o^2 = V \cdot r \tag{2.19}$$

Entropy $$\nabla s = o \tag{2.20}$$

In addition to the general assumptions listed above, Bastress also assumes,

1. There exists uniform contraction ratios for the stream lines.
2. The flow is hometropic.
3. The radial pressure gradient is zero.

The first assumption implies solid body rotation at each plane. This can be shown by considering the conservation of angular momentum for two streamlines within the flow.

On the j^{th} streamline, conservation of angular momentum gives,

$$\omega_o r_{oj}^2 = \omega_j r_j^2 \, . \tag{2.21}$$

On the $j + 1^{th}$ streamline, conservation of angular momentum gives,

$$\omega_o r_{oj+1}^2 = \omega_{j+1} r_{j+1}^2 \, . \tag{2.22}$$

Thus,

$$\omega_j = \omega_o \frac{r_{ojo}^2}{r_j^2} \, , \qquad \omega_{j+1} = \omega_o \frac{r_{oj+1}^2}{r_{j+1}^2} \tag{2.23}$$

Since the contraction ratios of each streamline are assumed constant,

$$\omega_o = \omega_j \cdot \frac{r_j^2}{r_{oj}^2} = \omega_{j+1} \frac{r_{j+1}^2}{r_{oj+1}^2} = \text{a constant with radius.} \qquad (2.24)$$

The second assumption leads to the conclusion that the stagnation temperatures and pressures should be considered constant normal to the streamlines. However, this violates the Crocco-Vaszonyi equation discussed earlier. This contradiction arises because a solid body vortex is in general rotational even when the gradient of the vorticity vector is zero, as is found in a Beltrami Helical motion.

The third assumption leads to the conclusion that centrifugal forces are negligible and that the thermodynamic variables may not vary with radius. An additional consequence of the second and third assumption is that the total velocity must be a constant in each plane normal to the axis.

Based upon these assumptions and the listed equations, Bastress developed an equation for the change in effective throat area with angular momentum of the flow. The axial velocity at the throat is given by,

$$w^* = (a_*^2 - \phi^{*2} r^2)^{1/2} \qquad (2.25)$$

where,

$\phi = (v - \omega_o r)$

a^* = the accoustic speed at the throat

ω_o = the initial spin rate

$$\frac{A^*_{eff}}{A^*} = \frac{1}{A^*}\int_0^{D^*/2} 2\pi r\left(1 - \frac{\phi^{*2} r^2}{a_*^2}\right)dr = \frac{2}{3\theta^2}\left[1 - (1-\theta)^{3/2}\right] \qquad (2.26)$$

where,

$$\theta = \phi^* D^*/2a^* = \left({}_oD^*/2a^*\right)\left[(D_o/D^*)^2 - 1\right] .$$

The properties of Eqn. (2.26) are such that as the spin rate, ω_o, goes to zero the ratio of the areas approach unity. The parameter θ has a maximum value of unity. At this point, the effective area reduction is two-thirds. When θ approaches unity, the axial velocity at the wall approaches zero. Thus, there is a limitation to the analysis in that the initial spin rate cannot exceed a certain value because of the initial assumption of uniform contraction ratios.

Bastress then relates the change in effective throat area to a change in chamber pressure using conventional internal ballistic relations. Thus, it is concluded that rotation can reduce the effective throat area, and thereby increase the chamber pressure and burning rate of the propellant as illustrated in Fig. 3.

2.3.4 Theory of Manda

An additional study related to the flow in a nozzle generated by an end-burning rocket motor is presented by Manda (8). In this work, certain improvements are made upon the theory of Bastress by including the radial momentum equation, thereby eliminating the necessity for the assumption of constant total velocity and the implied assumption of uniform thermodynamic properties across a plane. The assumption of uniform contraction ratio,

however, is retained.

The pertinent equations of this study are given below.

State $P = \rho R t$ (2.27)

Energy $c_p T_o = c_p t + \frac{w^2 + v^2}{2} = \text{const. on streamlines}$ (2.28)

Angular Momentum $Vr = \Gamma = \text{const. on streamlines}$ (2.28a)

Radial momentum $\frac{1}{\rho}\frac{\partial P}{\partial r} = \frac{V^2}{r}$ (2.29)

Entropy $\nabla s = o$

It might be pointed out that the lack of a continuity equation is replaced by the assumption of uniform contraction ratios which implies that all the flow in the chamber is conserved in the stream shells. Therefore, the location of the streamlines may be determined from the contraction of the nozzle wall.

By combining the equations for energy and angular momentum in a stream shell, along with an isentropic expansion from the chamber conditions (T_o, P_o), Manda obtains the following expression.

$$\frac{2g\gamma RT_o}{\gamma-1}\left(\frac{T}{T_o} - 1\right) + W^2 - W_o^2 + (r_o\omega)^2\left[\left(\frac{r_o}{r}\right)^2 - 1\right] = 0 \qquad (2.31)$$

Since the axial velocities eminating from the propellant surface are small, the axial velocity W_o^2 is subsequently neglected. Therefore, an expression for the axial velocity can be obtained.

$$W^2 = \frac{2gR\gamma T_o}{\gamma-1}\left(1 - \frac{T}{T_o}\right) - \omega_o^2\left(\frac{R_o}{R^*}\right)^2\left[\left(\frac{R_o}{R}\right)^2 - 1\right] r^2 \qquad (2.32)$$

where,

$$R_o/R = r_o/r$$

Manda next employs the radial momentum equation which is integrated assuming isentropic relations between the thermodynamic variables.

$$\frac{1}{\rho}\frac{\partial P}{\partial r} = \frac{V^2}{r} \tag{2.29}$$

Although not stated, this integration then implies the existence of a homentropic flow field. However, as in Bastress' analysis, this is a contradiction to the fact that a solid body vortex is rotational.

Thus, the following expression is obtained at the nozzle throat,

$$w^* = a_*^2 - \omega_o^2 (R_o/R^*) \left[2 \left(\frac{R_o}{R}\right)^2 - 1\right] r^2 \tag{2.33}$$

where R^* = radius of the geometrical throat

R_o = chamber radius

ω_o = the initial motor spin rate.

Substituting this expression into the equation for the axial velocity evaluated at the throat gives,

$$(P/P_o)^{\frac{\gamma-1}{\gamma}} = \left(\frac{T}{T_o}\right) = \frac{2}{\gamma+1} + \frac{\gamma-1}{2g\gamma R T_o}\left(\frac{R_o}{R_*}\right)^4 r^2 \,. \tag{2.34}$$

Manda then applies the result to an equation for the mass flow rate at the throat so that the effect of the initial angular momentum upon the mass flow rate can be determined.

$$w^{*2} = a_*^2 - \omega_o^2 \left(\frac{R_o}{R^*}\right)^2 \left[2 \left(\frac{R_o}{R^*}\right)^2 - 1\right] r^2 \qquad (2.35)$$

In conclusion, Manda finds that the mass flow rate can be significantly reduced for large values of initial angular momentum. However, the effect is reduced for a high flame temperatures of the propellant gases. Manda's results are presented in Fig. 4.

Summary

Recently, King (9) has published a discussion of the two analyses of end burning motors presented by Bastress and Manda. In this review, some of the contradictory statements and results of these analyses are discussed. King concludes that the basic error in the two analyses is the assumption of uniform contraction ratio. This assumption leads to an overspecification of the problem. This can easily be seen by summarizing the equations employed by each author.

Bastress

Equations	Unknowns
1. State	$p, \rho, t, u, v = f(r)$
2. Energy	
3. $\frac{\partial P}{\partial r} = 0$	
4. Angular Momentum	
5. Entropy, $vs = o$	

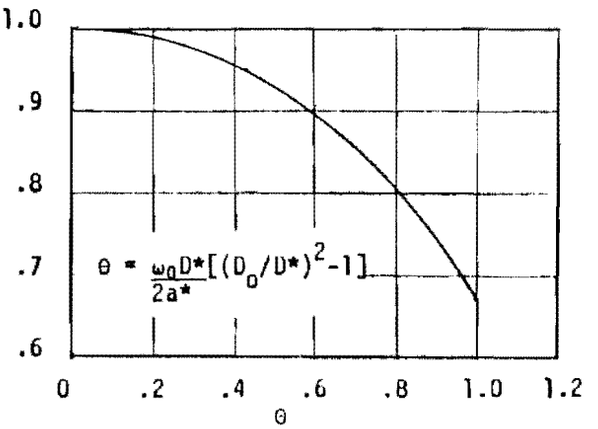

FIGURE 3 THE RESULTS OF THE THEORY OF BASTRESS(4).
(Taken from reference (4) , Bastress)

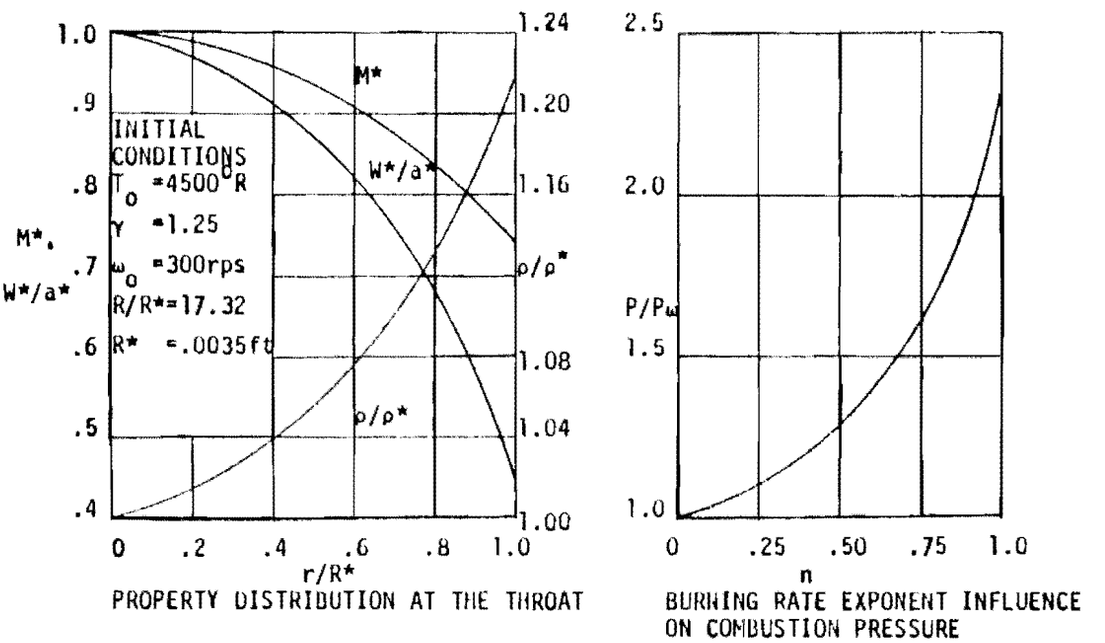

FIGURE 4 THE RESULTS OF THE THEORY OF MANDA(5).
(Taken from reference (5) , Manda)

Manda

Equations	Unknowns
1. State	p, ρ, t, u, v = f(r)
2. Energy	
3. Radial Momentum	
4. Angular Momentum	
5. Entropy, $\nabla s = 0$	

In addition to the equations listed, each analysis employs the assumption of uniform contraction ratios. As stated earlier, this assumption is equivalent to solid body rotation at every plane. Mathematically, this means that the dependent unknowns are reduced to four. Thus, it can be seen that there exists one too many equations for the number of dependent unknowns. Thus, each analysis is over-specified.

Further evidence of over specification is that each analysis employs a different set of governing equations. A consistent set of equations are given below.

1. State
2. Energy
3. Angular Momentum
4. Radial Momentum
5. Mass flow
6. Entropy

Thus, it can be seen that there are six equations and six unknowns which are a function of radius. Therefore, no assumptions are necessary regarding the nature of the tangential velocity (68).

In addition to the problem of overspecification, there is a contradiction in the treatment of the entropy of the flow. Each of the authors assumes a homentropic flow field either by implication or direct statement. However, it was shown in an earlier section that a solid body vortex is rotational in nature. Hence, a variation in the entropy normal to the streamlines is necessary. An additional consequence of the rotational nature of the flow is that the stagnation properties must vary normal to the streamlines.

Thus a complete approach to the problem must include entropy gradients and the existance of stagnation property variations normal to the streamlines.

3. VORTEX FLOWS IN ROCKET MOTOR CHAMBERS

3.1 Introduction

The properties of the flow in a rocket motor chamber are very important to the overall study of vortices in rotating rocket motors, since these properties serve as initial conditions for the flow in the nozzle. In addition, the flow field in the chamber provides information as to the effects of the vortex on propellant burning.

In general the vortex flow in an end-burning motor is easily described, since in that case the flow is generated with a solid body vortex. Under ideal conditions this solid body vortex would travel down the chamber and enter the nozzle without deformation. The action of viscosity would not necessarily disrupt the solid body vortex since, when the walls are rotating, there is no tangential velocity boundary layer at the walls. Although the solid body vortex is considered to be an equilibrium flow, it is not necessarily stable to disturbances (53). Recently, Hall (10) presented indications that instabilities may develop if gradients in the axial velocity are present.

In the case of an internal-burning cylindrically perforated core, the theory is considerably more complicated. In the ideal, inviscid case, a free vortex pattern would be established since every particle of gass is generated at the same radial location and thus has the same angular momentum. When the gases flow radially inward, the tangential velocity must increase to conserve angular momentum. This leads to the formation of a void core of zero temperature and pressure which is a necessary consequence if the tangential velocity

reaches the maximum isentropic speed.

The more complex grains such as the star, the wagon wheel and the dendrite add considerable difficulty. The mass generated at various radii from the axis would not possess a unique value of angular momentum. Also, there could exist variations in the burning rate due to stagnation of the faster moving gases on the fingers of the grain and pressure variation in the radial direction balancing the acceleration forces.

When viscous forces are considered, the ideal vortex is upset. This occurs because the tangential shear stress increases as radius decreases. At the centerline, which is a free boundary, there can be no shear moment. Therefore, a solid body vortex is established close to the axis which extends out some distance into the chamber and merges with the free vortex.

3.1.1 Theory of Burgers

In 1940 and 1948, Burgers (11, 12) discussed an exact solution to the Navier-Stokes equations for the three-dimensional vortex flow of an incompressible, viscous fluid.

The basis for this solution rests upon the assumption that the axial velocity varies with axial distance only.

$$w = a \cdot z \tag{3.1}$$

Then, employing the continuity equation,

$$\frac{\partial w}{\partial z} + \frac{1}{r} \frac{\partial ru}{\partial r} = 0 \tag{3.2}$$

the radial velocity becomes,

$$u = - ar + K/r \tag{3.3}$$

where K is a constant of integration which may be a function of z only. K is then eliminated on the grounds of the finiteness of the radial velocity at the centerline.

$$u = - ar \tag{3.4}$$

The radial and axial momentum equations are satisfied by the above expressions. The tangential momentum equations for axisymmetric time independent flow is,

$$- Ar \frac{\partial V}{\partial r} - AV = \nu\left(\frac{\partial^2 u}{\partial r^2} + \frac{1}{r}\frac{\partial u}{\partial r} - \frac{u}{r^2}\right) , \tag{3.5}$$

where ν = kinematic viscosity.

$$A = \frac{\dot{m}_o/L}{\text{Area} \cdot \rho} = \text{const.}$$

$\dot{m}/L$ = mass per unit length

The following solution was obtained for Eq. (3.5).

$$V = \frac{\Gamma}{2\pi r}\left(1 - e^{-A\, r^2/2r}\right) \tag{3.6}$$

$$\Gamma = 2\pi\, V \cdot r$$

where Γ is the circulation about the axis.

The vorticity is given by

$$\bar{\omega} = \frac{A\,\Gamma}{2\pi\nu} e^{Ar^2/2\nu} \tag{3.7}$$

The total dissipation per unit length of Z is given by

$$\phi = \rho \nu \int_0^\infty dr\, 2\pi r\gamma^2 = \rho \frac{Ar^2}{4\pi} \tag{3.8}$$

It can be seen that the dissipation is independent of viscosity and proportional to the third power of the tangential velocities.

Burgers thus obtained an exact solution for a three-dimensional vortex flow. The results are completely analytical and are therefore quite useful. An actual flow whose axial velocity varies linearly with axial position while the tangential and radial velocities vary only with radial position may not be physically realizable. However, it may approximate a psuedo one-dimensional flow with rotating boundaries through which mass is injected.

Rott (13, 14) has considered Burger's solution in more detail by allowing the velocity profiles to vary with time. He also has calculated the resultant pressure and temperature distributions.

3.1.2 Theory of Einstein and Li

In 1951, Einstein and Li (15) studied the flow in an emptying container filled with a liquid. The model for the analysis was essentially that of an incompressible, viscous, steady, axisymmetric flow. It was assumed that the average axial velocity u was small while the variations in the axial velocity could be significant. The flow field was divided into two portions. A core having the same radius as the drain opening was assumed in which the volummetric flow rate was given by

$$Q = Q_o\, r^2/r_o^2 \tag{3.9}$$

where,

r_o = drain radius

$Q_o \equiv$ The total volumetric discharge rate.

In the remainder of the flow field, from the drain radius to the outer walls,

$$Q = Q_o = \text{const.} \qquad (3.10)$$

R = The cylinder radius

In addition, it was assumed that,

$u = u(r)$ $\qquad u^2 << v^2$

$v = v(r)$ $\qquad w^2 << v^2$

$w = 0 \; ; \quad r > r_o$

Einstein and Li found that in the core region,

$$v = \frac{v_o \, r_o}{r} \, \frac{(1 - e^{A/2(r/r_o)^2})}{(1 - e^{-A/2})} \qquad (3.11)$$

where,

$A = (Q_o/2\pi\gamma\nu)$

v_o = The tangential velocity of the cylinder

ν = The kinematic viscosity

In the outer region the tangential velocity is given by,

$$V = \left(\frac{V_o R_o}{r}\right) \left| \frac{(A-2)(1 - e^{A/2(r/r_o)^2})}{A(1 - e^{-A/2} \cdot (\frac{r}{R})^{A-2}) - 2(1 - e^{-A/2})} \right| , \quad A \neq 2$$

$$V = \left(\frac{V \cdot R}{r}\right) \left| \frac{A - 2(1 - e^{-A/2})(1 - (\frac{r}{R})^{-(A-2)})}{A(1 - e^{-A/2} \frac{r}{R}^{(A-2)}) - 2(1 - e^{-A/2})} \right| , \quad A = 2 \qquad (3.12)$$

In addition to these laminar flow cases, Einstein and Li also set up the equations for the turbulent motion of the vortex. They concluded that a solution equilivant to the laminar case could be obtained if the constant A is redefined to be,

$$A_e = Q_o/2\pi\varepsilon(\xi + \nu) \qquad (3.13)$$

where,

$$\varepsilon_r \frac{\partial}{\partial r} (v/r) = - \overline{(u'v')} \qquad (3.14)$$

3.1.3 Theory of Donaldson

In a Ph.D. thesis (16) and other reports (17, 18), Donaldson presents a rather complete review of the solutions for the Navier-Stokes equations for viscous, incompressible, driven vorticies which have been accumulated over the years. He also presents a great deal of the theory and equations for such motions in general form.

His contribution to the theory of viscous vortex motion is the study of the Navier-Stokes equations for a three-dimensional vortex whose tangential velocity component is a function of the radial coordinate only.

Under the above catagory, two families of solutions were studied. They are,

1. $w = k \circ f(r)$ (3.15)

2. $w = k \cdot z \cdot f(r)$ (3.16)

The following physical interpretation of the above families of solutions were given. The first family is a limited one since any mass added at the boundaries must be absorbed by a sink at the centerline. However, the second family where

$$w = k \cdot z \cdot f(r) \tag{3.17}$$

may be interpreted as a pseudo, two-dimensional problem where mass is added through a rotating container and is uniformly distributed in the flow field.

When the axial velocity is of the form

$$w = k_1 \cdot z \cdot f_1(r) + k_2 f_2(r) \tag{3.18}$$

Donaldson shows that the only consistent forms of the tangential and radial velocities are,

$$\begin{aligned} u &= u(r) = w\, g\,(x) \\ v &= v(r) = V_0\, h\,(x) \end{aligned} \tag{3.19}$$

where,

V_0 = The tangential velocity at the wall

$x = \frac{r}{R}$

$g(x)$ = An arbitrary function of radius for the radial velocity

$h(x)$ = An arbitrary function of radius for the tangential velocity

R = The radius of the rotating cylinder

Choosing only the first portion of the general expression for the axial velocity,

$$\frac{wz}{R} f(x) \tag{3.20}$$

and substituting the above expression into the continuity equation gives,

$$\frac{1}{x} \frac{d}{dx} (xg) = - f \ . \tag{3.21}$$

The general expression for the velocities may then be substituted into the axial momentum equation,

$$\frac{\partial P}{\partial z} = \rho \frac{\omega^2}{R} \left(\frac{z}{R}\right) \left[- gf' - f^2 + \frac{\nu}{WR} \left(f'' + \frac{f'}{x}\right)\right] \ . \tag{3.22}$$

Integrating,

$$P = 1/2 \ \rho\omega^2 \left(\frac{z}{R}\right)^2 \left[- gf' - f^2 + \frac{1}{Nw} \left(f'' + \frac{f'}{x}\right)\right] + i(x) \tag{3.23}$$

where,

$i(x)$ = a constant of partial integration

$Nw = WR/\nu$.

Substituting the general velocity equations into the radial momentum equations shows that

$$\frac{\partial P}{\partial r} = \text{function of x alone} \ . \tag{3.24}$$

Therefore,

$$- gf' - f^2 + \frac{1}{Nw} \left(f'' - \frac{f'}{x}\right) = \text{const.} = c \ . \tag{3.25}$$

In which case,

$$\frac{\partial P}{\partial r} = 0 + \frac{\partial i(x)}{\partial r} = \text{function of x alone} . \tag{3.26}$$

The function g(x) may be eliminated from Eq. (3.25) by substituting the continuity relationship, Eq. (3.21)

$$f'f''' - (f'' - f'/x)[f'' - Nw(f^2 - c)] - Nw\, f(f')^2 = 0 \tag{3.27}$$

Donaldson sets up a general solution for the differential equations given in Eq. (3.27). For the case of an infinite, rotating, porous cylinder, the boundary conditions are,

$$f(o) = 1, \quad f'(o) = 0, \quad f(1) = 0 \tag{3.28}$$

in which case,

$$C = - (R/z) \cdot (R/\rho\omega^2) \cdot (\frac{\partial P}{\partial z}) .$$

The constant C may be determined from the boundary conditions as follows.

$$C = f^2(o) - \frac{1}{Nw} [f''(o) + \lim_{x \to 0} (\frac{f'(x)}{x})] . \tag{3.29}$$

By examining the limiting process in Eq. (3.29),

$$\lim_{x \to 0} (\frac{f(x)'}{x}) = f''(o) . \tag{3.30}$$

the following result was obtained.

$$C = 1 - 2/Nw\, f''(o) . \tag{3.31}$$

Now the Eq. (3.27) can be written,

$$f'f'' - (f'' - f'/x)[f'' - 2f''(o)] + Nw(f^2 - 1)(f'' - f'/x) - Nw\, f(f')^2 = 0 \tag{3.32}$$

Donaldson investigated a number of limiting solutions.

1. $N_w = 0$

2. $N_w = \pm \infty$ 2a. Blowing at the walls

3. $N_w = -\infty$ 3a. Suction at the walls

1. When $N_w = 0$, $\nu = \infty$

$$f'f'' - (f'' - f'/x)[f'' - 2f''(o)] \tag{3.33}$$

It was found that there are an infinite number of solutions.

$$f(x) = 1 - x^{2m} \qquad m = 1, 2, 3 .... \tag{3.34}$$

However, the only physically possible solutions is,

$$f(x) = 1 - x^2 \tag{3.35}$$

2. When $N_w = \pm \infty$, $\nu = 0$

$$(f^2 - 1)(f'' - f'/x) - f(f'^2) = 0 \tag{3.36}$$

In this case, the number of boundary conditions must be reduced, since the second order derivatives were eliminated,

$$f(o) = 1 ; \qquad f'(o) = 0 \tag{3.37}$$

The general form of the solution in this case is

$$f(x) = \cos(ax^2) \tag{3.38}$$

Since the viscosity has been eliminated, the axial velocity may have any desired value at the bounding walls, except when blowing occurs, in which

case the axial velocity is zero. The simplest of all solutions is that when a = 1. Then, f = 1 for both suction and blowing.

2a. Blowing at the Walls $N_w = -\infty$, $v = 0$

Since in blowing, the flow is aware of the presence of a boundary, the constant, a, must be chosen so that the axial velocity is zero at the wall despite the vanishingly small viscosity. Thus, there may be patterns of alternating forward and reverse flow for the axial velocity.

$$w = W \frac{z}{R} \cos\left[\left(\frac{2n+1}{2}\right) \pi x^2\right] \tag{3.39}$$

2b. Suction at the Walls $N_w = -\infty$, $v = 0$

$$f = \cos(ax^2) \tag{3.40}$$

In this case the constant, a, may be chosen to have any value desired. In general, however, the form of the solution is the same as for the blowing at the wall case except that the requirement for the axial velocity to vanish at the wall may be removed. One additional point arises, however, because when the magnitude of the suction is large, the pressure gradient may be adverse to the net mass flow so that any number of inward and outward flow cells may be present. Some of the results of these studies are presented in Fig. 5.

3.1.4 Theory of Lay

A paper was published by Lay (19, 20) in 1959 for the flow in a tube with superposition of the free vortex onto a uniform axial flow. The

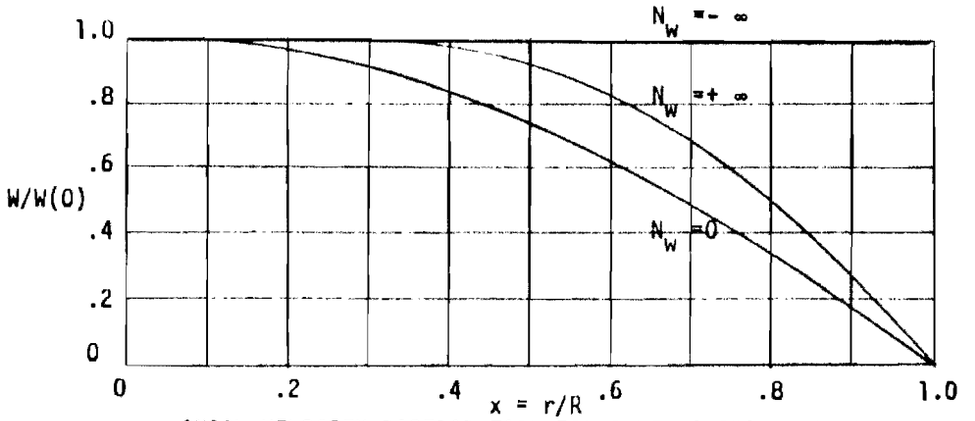

AXIAL VELOCITY DISTRIBUTION FOR SOME LIMITING CASES

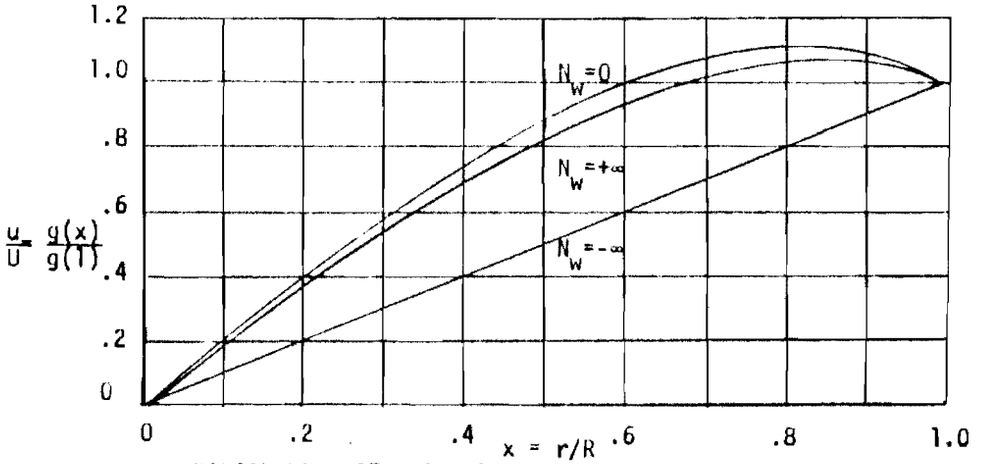

RADIAL VELOCITY DISTRIBUTION FOR SOME LIMITING CASES

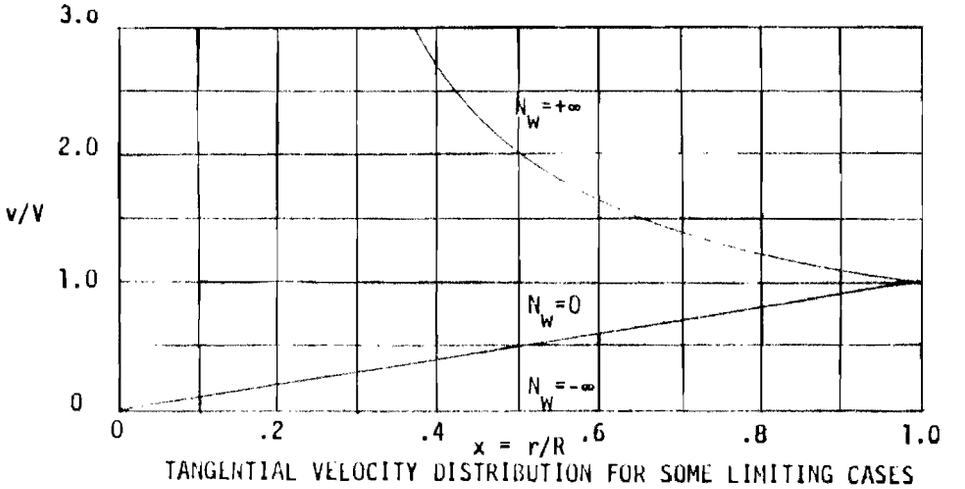

TANGENTIAL VELOCITY DISTRIBUTION FOR SOME LIMITING CASES

FIGURE 9 SOME RESULTS OF THE THEORY OF DONALDSON.(16)
(Taken from reference (16) , Donaldson)

analysis is strictly applicable for inviscid, irrotational, flows since velocity potentials are employed. However, compressibility effects are included.

The familiar axisymmetric velocity potential and stream function equations are derived for the case of tangential and radial velocities only. These two sets of equations are then combined under the hodograph transformation.

$$\begin{aligned} v &= q\cos\theta = \frac{\partial\phi}{\partial x} \\ u &= q\sin\theta = \frac{\partial\phi}{\partial y} \end{aligned} \tag{3.41}$$

The equations are then, in terms of the unknowns,

$$\psi = \psi(q,\theta) \tag{3.42}$$

where,

q = the velocity

θ = angle of the velocity vector

The superposition of the axial flow is achieved by assuming a sink flow in two dimensions combined with a uniform axial velocity which does not alter the sink flow pattern. It was possible to arrive at the sink flow vortex flow field from the velocity potential and the stream function equations when transformed by the hodograph transformation. This sink flow vortex was then uniformly translated by superposition of a constant axial velocity.

In conclusion, the direction of the streamlines were determined for the superposition of a sink flow vortex under uniform translation. The

position of the radius of maximum isentropic speed was also calculated.

3.1.5 Theory of Pengelly

Pengelly (21) in 1957 presented an analysis of a two-dimensional, compressible, viscous vortex. The radial velocity was assumed to be small compared to the tangential velocity and heat transfer was neglected.

The model for the flow consists of a rotating, porous container. The gases leave the cylinder wall with a combined radial and tangential velocity. A schematic of the physical model for this theory is presented in Fig. 6. The gases then spiral inward to a radius where the viscous stresses are zero, at which point the radial flow is converted to an axial flow and exhausted out of the chamber. Another possibility lies in the removal of the incoming mass by slots at the end wall. Thus, the flow field can be treated as a truly two-dimensional flow. Therefore, the mass flow rate is given by,

$$\dot{m} = \rho u L 2\pi r \tag{3.43}$$

where

L = the length of the chamber.

All gradients with respect to z and θ are zero. Therefore, the following form of the Navier-Stokes equations can be written.

$$\sigma(du/dr + v/r) + r d^2v/dr^2 + (dv/dr - v/r) \tag{3.44}$$

$$dP/dr = (\rho v^2/r)\ \{1 + (u^2/v^2)(1 + \frac{d\rho/dr}{\rho/r}) \tag{3.45}$$

where

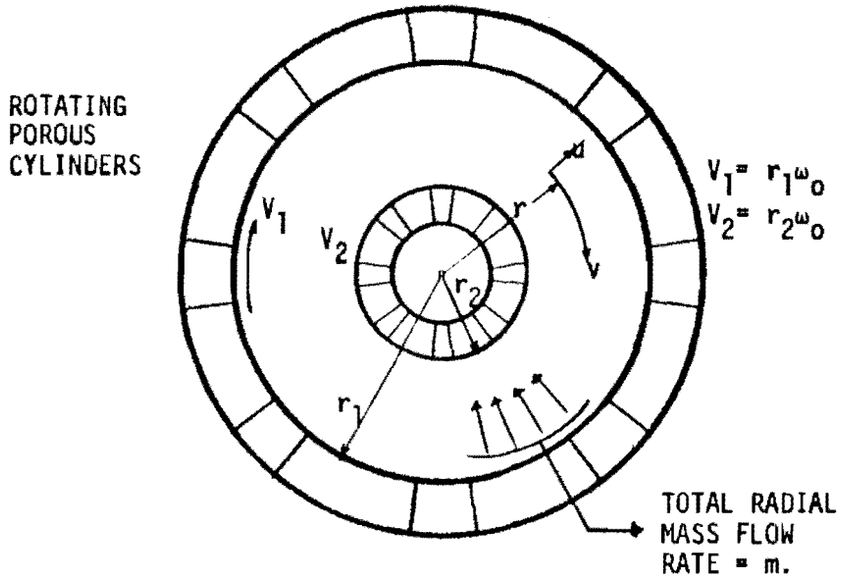

TWO DIMENSIONAL VISCOUS VORTEX FLOW FIELD

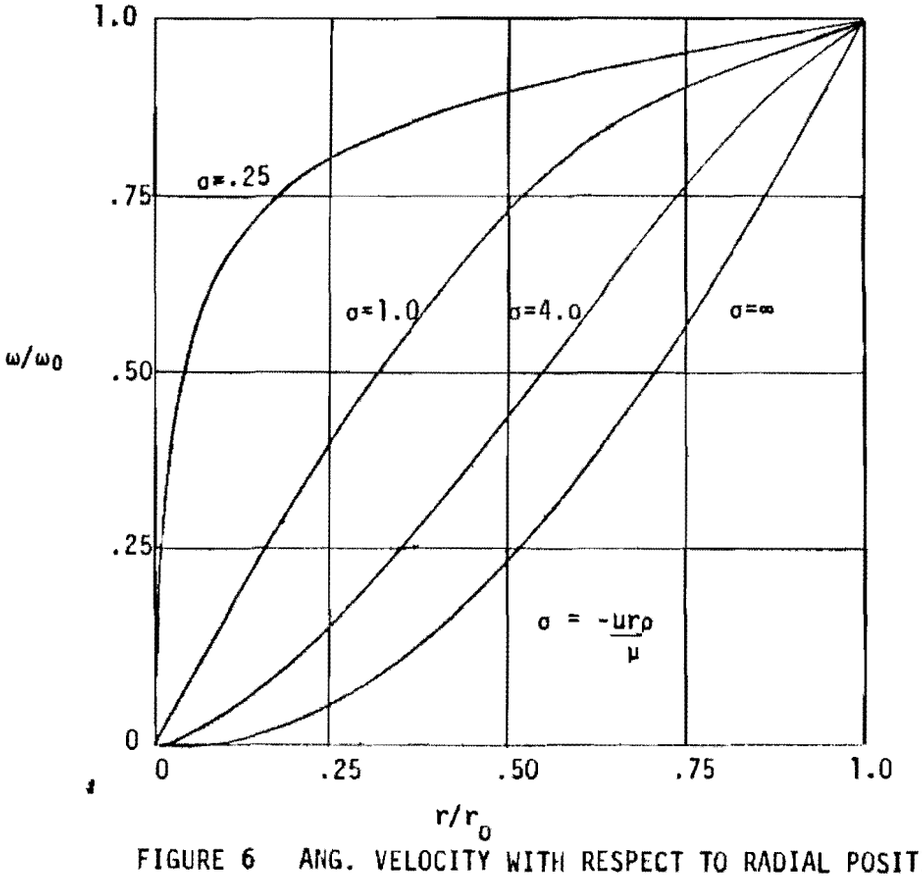

FIGURE 6 ANG. VELOCITY WITH RESPECT TO RADIAL POSITION FOR SEVERAL VALUES OF FLOW RATIO ,σ .
(Taken from reference (21) , Pengelly)

$$\sigma \equiv \frac{ur\rho}{\mu} .$$

In addition, the energy equation is given by

$$\frac{dT_s}{dr} = \frac{1}{c_p} \left\{ \frac{1}{\rho} \frac{dP}{dr} - \frac{r\phi}{\mu\sigma} + \nu \frac{dv}{dr} \left(1 + \frac{u^2}{r^2}\right) + \frac{v^2}{2} \frac{d}{dr} \left(\frac{u}{v}\right)^2 \right\} \tag{3.46}$$

where,

ϕ = the dissapation function

$$\phi = \mu \left(\frac{V}{r}\right)^2 \left[\left\{ \frac{dv/dr}{v/r} - 1 \right\}^2 + \left(\frac{u}{v}\right)^2 \left\{ \left(\frac{du/dr}{u/r}\right)^2 - \frac{du/dr}{u/r} + 1 \right\} \right] \tag{3.47}$$

T_s = the stagnation temperature.

The above equations are exact under the listed assumptions for the case of a two-dimensional vortex. Equation (3.44) can be integrated without approximation for the case of σ equal to a constant to give the following results.

$$\Gamma = A - B/r^{\sigma-2} \qquad \sigma \neq 2$$

$$\Gamma = A_2 - B_2 \ln r \qquad \sigma = 2$$

$$v = \Gamma/2\pi r \ .$$

The remaining conservation equations can be integrated provided that

$$u^2 << v^2,$$

so that,

$$\phi = \mu \left(\frac{v}{r}\right)^2 \left\{ \frac{dv/dr}{v/r} - 1 \right\}^2 \tag{3.48}$$

The results of a numerical example show that, under certain conditions, the action of the viscous forces can decrease the stagnation temperature

near the centerline as is found in the Ranque-Hilsch vortex tube. It should be emphasized that the theory is applicable only to a two-dimensional vortex with laminar flow. The mass input is exhausted out of the cylinder either through slots in the end walls, or axially through some small hole on the centerline.

Pengelly also discusses the possibility of applying the above analysis to the turbulent case. He concluded that it may be possible if some effective turbulent viscosity can be determined which can be employed in the radial Reynolds number.

3.1.6 Theory of Deissler and Perlmuter

In 1958, Deissler and Perlmuter (22) presented an analysis of the flow in a vortex tube. The model chosen for study was incompressible, steady, viscous, three-dimensional flow. It was assumed that the tangential and radial velocities were functions of radius only. Then it was shown that only a linear variation of axial velocity with axial position is consistent with these assumptions. (See Fig. 6).

The variation in axial velocity was assumed to be uniform in both a core region and an outer region. However, a step variation in the velocities was allowed between these regions.

Based upon this model, the authors were able to determine the form of the tangential velocity as a function of radius and several other parameters. The complete tangential momentum equation is given by,

$$\rho u \frac{\partial v}{\partial r} + \rho w \frac{\partial v}{\partial z} + \rho \frac{uv}{r} = \frac{\partial}{\partial z}\left(\mu \frac{\partial v}{\partial z}\right) + \frac{\partial}{\partial r}\left[\mu \left(\frac{\partial v}{\partial r} - \frac{v}{r}\right)\right] + \frac{2\mu}{r}\left(\frac{\partial v}{\partial r} - \frac{v}{r}\right) . \qquad (3.49)$$

Under the assumption that V = v(r) and μ = constant, Eq. (3.49) can be written as,

$$\rho u \frac{\partial v}{\partial r} + \rho \frac{uv}{r} = \mu \left(\frac{d^2v}{dr^2} + \frac{1}{r}\frac{dv}{dr} - \frac{v}{r^2}\right) \quad . \tag{3.50}$$

Therefore, since the product ρu is a function of radius only, the general solution is,

$$V = \frac{C_1}{r} \int r_e \int \frac{\rho u}{\mu} dr \, dr + C_2/r \tag{3.51}$$

Where C_2 = 0 for finiteness of velocity at r = 0. The particular solutions for the core region and the outer region are then determined by numerical integration.

In addition to the above kinematic study, the energy equation was also solved assuming that the temperature is a function of radius only. The solution for tangential velocity and temperature are given as a function of radius in terms of the following parameters.

r_o/r_i = the ratio of the assumed core radius to the cylinder radius

w_c/w = the ratio of the core mass flow to the total mass flow

R_e = the radial Reynolds number

The results indicate that with high Reynolds numbers the flow becomes increasingly in the nature of a free vortex. However, there always remains a small region near the centerline of solid-body vortex motion which grows as the Reynolds number decreases. The effect of w_c/w is not great when the Reynolds number is large. When w_c/w is small and the Reynolds number is small, the flow tends to be more free vortex in nature.

The temperature distributions show that there is very little energy separation except at the lowest Reynolds numbers. This suggests that the observed energy separation in the Ranque-Hilsch tube experiments must be attributed to turbulence effects which would essentially increase the apparent viscosity of the flow. Therefore, a turbulent model was proposed based upon the additional assumption of a constant eddy viscosity. This made no change in the velocity distribution for a given Reynolds number. For the calculation of the turbulent temperature distribution, it was necessary to make the following assumptions.

$$\mu = \rho\varepsilon$$

$$k = \rho \, cp \, \varepsilon_H$$

$$\varepsilon = \varepsilon_H$$

An additional term was then added to account for the effect of the radial pressure gradient upon the turbulent heat transfer.

In conclusion, the turbulent temperature analysis was shown to agree with experimental vortex tube data when the proper choice of the eddy viscosity was made. Essentially, the effects of the increased viscosity and the radial pressure gradient upon the turbulent heat transfer allowed a greater energy separation, thus, a better correlation with experimental measurements.

3.1.7 Theory of Sullivan

In 1959, Sullivan (23) reported upon an analog to Burger's solution (ref. 11, 12) which is characterized by the existance of two cells. In

this model, the flow does not spiral toward the axis then out along it, but has a central region of reverse flow. This solution came about during the course of an investigation of the complete family of solutions based upon velocity profiles of the following form in an incompressible, viscous, steady, axisymmetric flow field.

$$\begin{aligned} u &= u(r) \\ v &= v(r) \\ w &= k \cdot z \cdot \bar{w}(r) \ , \end{aligned} \tag{3.52}$$

The particular solution in this report is for the case of an infinite rotating porous container through which liquid is flowing. The radial and tangential velocities and their derivatives are required to vanish at the centerline. At the container walls the velocity of the boundary and the tangential velocity are the same.

The two cell solution solution arises from the case where the radial Reynolds number approaches minus infinity. Physically, this means that large inward radial velocities exist at the container walls so that the inertial forces are much larger than the viscous forces. The following solution was obtained.

$$u = - ar + 6\ (\nu/r)[1 - e^{-(ar^2/2\nu)}] \tag{3.53}$$

$$w = 2az\ [1 - 3\ e^{-(ar^2/2\nu)}] \tag{3.54}$$

$$v = \Gamma/2\pi r\ [H(ar^2/2\nu)/H(\infty)] \tag{3.55}$$

$$H(x) = \int_0^x \exp\ \{- 5 + 3 \int_0^t \frac{(1-e^{-\tau})}{\tau}\, d\tau\} dt \tag{3.56}$$

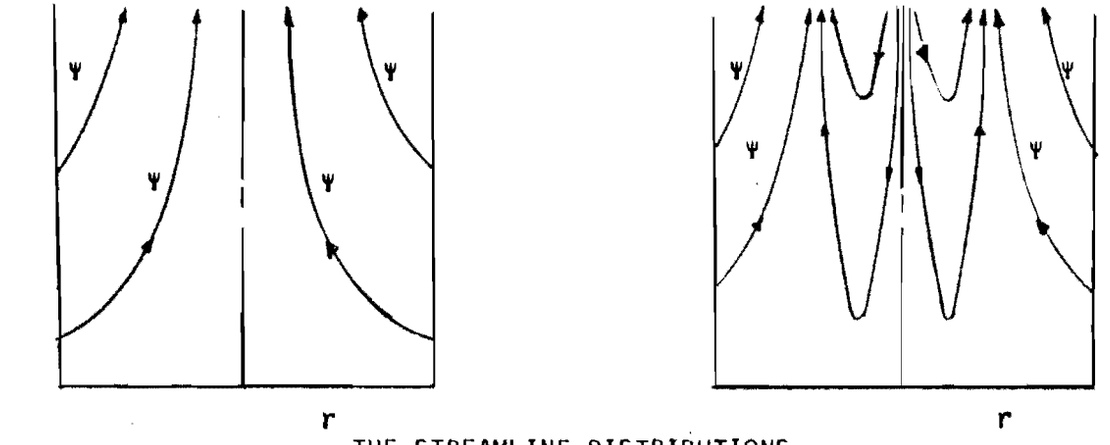

THE STREAMLINE DISTRIBUTIONS

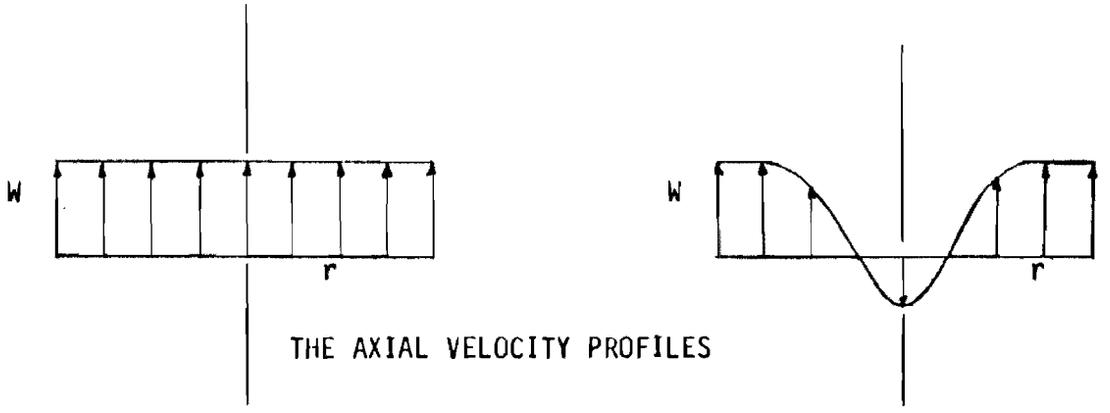

THE AXIAL VELOCITY PROFILES

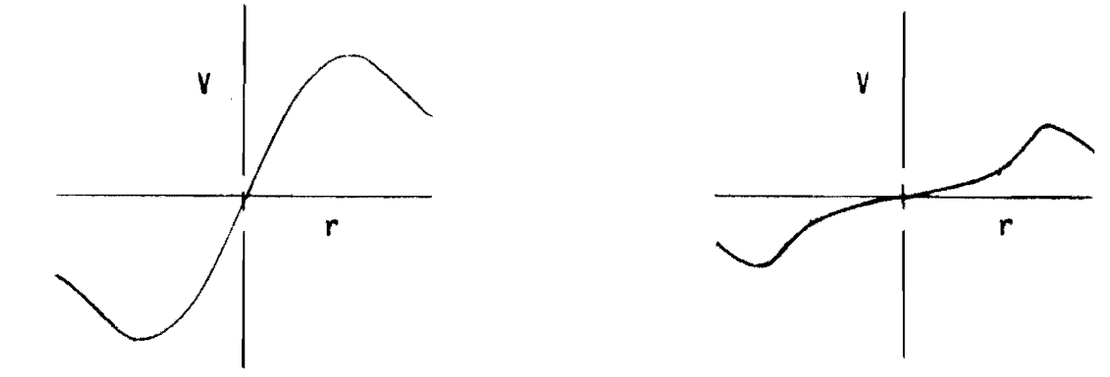

THE TANGENTIAL VELOCITY PROFILES

BURGERS' SOLUTION SULLIVAN'S SOLUTION

FIGURE 7 A COMPARISON OF THE THEORY OF BURGERS AND SULLIVAN
(Taken from reference (27), Lewellen)

Sullivan compares this solution to that of Burger and finds that, although the velocity expressions are different, the axial pressure gradients and dissipation are the same. Thus,

$$\partial P/\partial \tau = -4\, a^2 \rho z$$
$$\phi = \frac{\rho A \Gamma^2}{4\pi} . \tag{3.57}$$

The radial pressure function is, in general, quite different,

$$P = P_o - \rho/2 \{4\, a^2 z^2 + a^2 r^2 + 36(\nu^2/r^2)[1 - e^{ar^2/2\nu}]^2\} + \rho \int_o^r (\nu^2/r^2) dr \tag{3.58}$$

whereas Burgers and Rott (11, 12, 13, 14) found,

$$P = P_o - (\rho/2)[4\, a^2 z^2 + a^2 r^2] + \rho \int_o^r (u/r)^2\, dr . \tag{3.59}$$

3.1.8 Theory of Sibulkin

In a series of three articles (24, 25, 26), Sibulkin presents a method of analyzing certain vortex flows. The basis of the method is to establish the unsteady equations of tangential and radial momentum for viscous flow and the energy equation allowing radial transfer of energy only.

Radial Momentum

$$\rho r \omega^2 = \partial P/\partial r \tag{3.60}$$

Tangential Momentum

$$\frac{\partial \omega}{\partial t} = \frac{\nu}{r^3} \frac{\partial}{\partial r} \left(r^3 \frac{\partial \omega}{\partial r}\right) \tag{3.61}$$

Energy

$$c_p \frac{\partial T_\tau}{t} = c_p \frac{\partial T}{\partial \tau} + \frac{\partial (\frac{v}{2})^2}{\partial t} =$$

$$= \frac{1}{\rho} \frac{\partial P}{\partial z} + \frac{\nu}{r} \frac{\partial}{\partial r} [r^3 \frac{\partial \omega^2/2}{\partial r}] + \frac{k}{\rho r} \frac{\partial}{\partial r} (r \frac{\partial t}{\partial r}) \qquad (3.62)$$

The restrictions on these equations are:

1. $M << 1$
2. $u = 0$
3. Only radial energy transfer is allowed
4. Laminar flow
5. Axial and radial shear forces neglected.

The initial conditions for the problem are that of given initial property profiles determined from experiment.

The analytical approximation to these initial conditions are a quiescent core of zero temperature, pressure, and velocity, with a free vortex distribution around it. These initial conditions are gradually smoothed out as the integration in time proceeds. The boundary conditions in time and radius are:

$$\frac{\partial \omega}{\partial r} (0,t) = 0 \qquad \frac{\partial t_\tau}{\partial r} (0,t) = 0$$

$$\omega (R,t) = 0 \qquad \frac{\partial \tau_t}{\partial r} (R,t) = 0 \qquad (3.63)$$

τ_t = the total temperature.

These boundary conditions are for a stationary tube which extends to infinity. The axial position then is some function of time. These

equations were solved simultaneously by finite difference methods. The results indicate that the tangential velocity decays in time while the pressure gradient of the imposed inlet profile is gradually smoothed. The total temperature peak, however, indicated a gradual tendency to move inward. The initial conditions and some results are presented in Fig. 7.

3.1.9 Theory of Lewellen

In 1962 and 1964, Lewellen (27, 28) investigated the properties of real vortices contained in cylinders with small axial flow. The type of flow considered is one with strong circulation wherein the radial velocities are small compared to the tangential velocity as illustrated in Fig. 8. These solutions are compared to those of Donaldson (16), Sullivan (23), Burgers (12), and Rott (13). The above authors investigated exact solution to the Navier-Stokes equations when the following conditions hold.

$$W(r,z) = K_1 \circ z \circ f_1(r) + K_2\, f_2(r) \tag{3.64}$$

where,

$$u = u(r)$$

$$v = v(r) \ .$$

These analyses may be contrasted to those of Einstein and Li (15), and Deissler and Perlmutter (22), where approximate techniques were employed.

The assumptions leading to solutions of the three-dimensional flow in the analyses listed above are that,

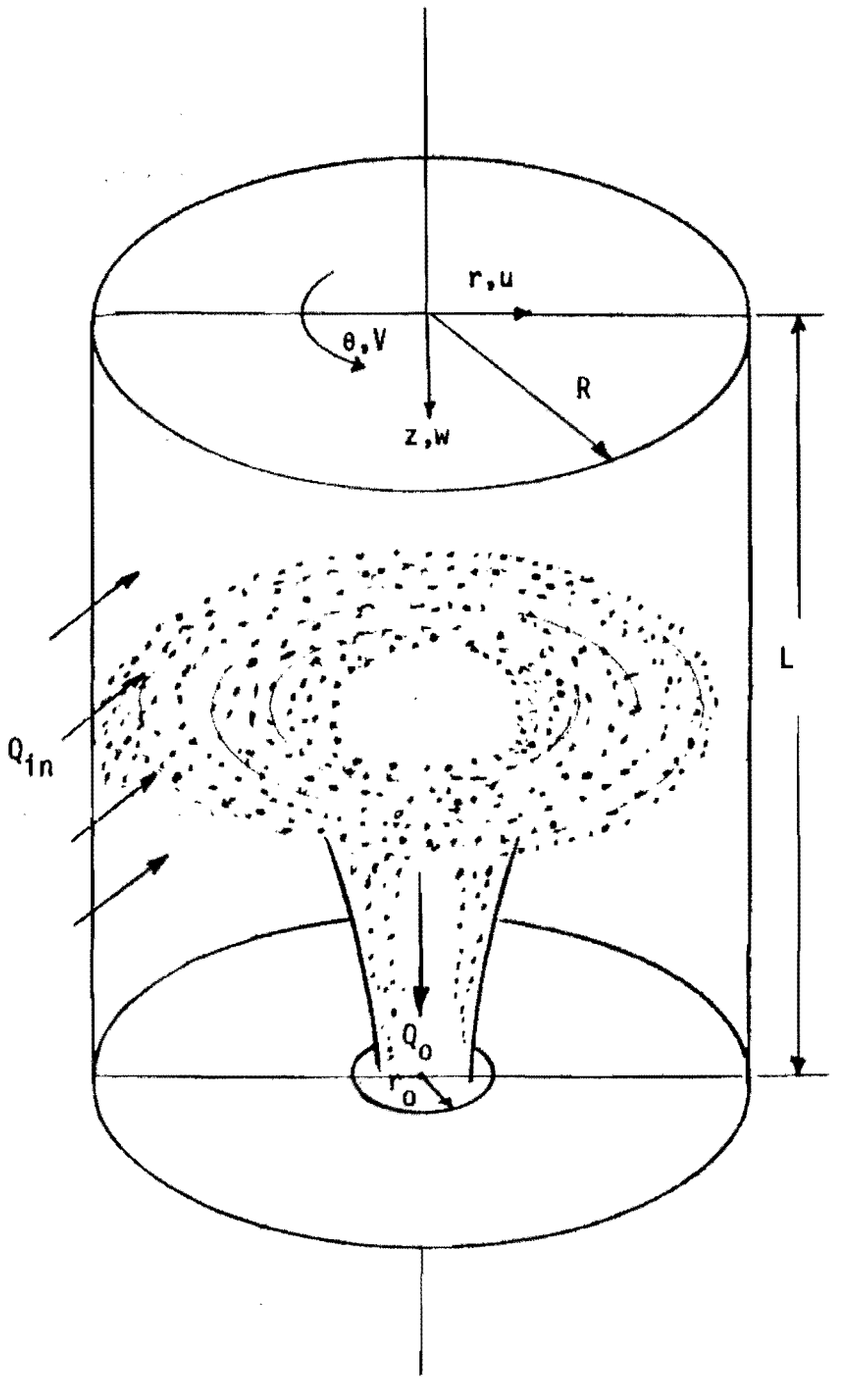

FIGURE 8 A DRIVEN VORTEX IN A CYLINDRICAL CONTAINER
(Taken from reference (28) , Lewellen)

$$
\begin{aligned}
w^2 &<< v^2 \\
u^2 &<< v^2 \\
u &= u(r) \\
v &= v(r) \ .
\end{aligned}
\tag{3.65}
$$

These approximations are justified when the axial velocity of the flow is small and the circulation is large. In the present paper, Lewellen attempted to bridge the gap of these two methods of attack and to point out the consequences of each approach. He took the complete Navier-Stokes equations for axisymmetric, viscous, laminar, incompressible, steady flow in cylindrical coordinates and employs the concept of the stream function to eliminate the continuity equation. The remaining equations were then written in terms of,

$$
\begin{aligned}
\Gamma &= vr = \Gamma(r,z) \\
\psi &= \psi(v,z) = \text{The stream function}
\end{aligned}
\tag{3.66}
$$

where pressure is eliminated by cross differentiation of the axial and radial momentum equations. Lewellen then derived the equations pertinent to the analyses of Donaldson and Sullivan (16, 23). He showed that the solutions given by Donaldson and Sullivan are not applicable to the analysis of the radial sink flow to a small opening in a cylindrical tank. However, by assuming pertibations in the Donaldson and Sullivan analysis to include small changes of ψ with axial position, Lewellen showed that when the circulation is large, there can be large changes in the stream function ψ.

To investigate this case, Lewellen expanded the expressions for the circulation and the stream function in the following manner.

$$\Gamma = \sum_{n=0}^{\infty} \Gamma_n(\eta,\zeta)e^n \qquad \text{where } \eta = (r/r_o)^2$$

$$\psi = \sum_{n=0}^{\infty} \psi_n(\eta,\zeta)e^n \qquad \zeta = z/l \tag{3.67}$$

The solutions thus obtained are valid for variations of the radial pressure gradient and axial velocities and therefore are not necessarily specified a priori. However, the solutions are quite dependent upon the boundary conditions of the stream function which in physical cases, must be related to the boundary layer phenomenon associated with the end section of the container. It is noted that in most real cases, the boundary layer must be solved to give proper initial conditions for the calculations, and some consideration should be given to the recirculation induced by the exhaust.

3.1.10 Lewellen 1965

In this paper, as in earlier papers, Lewellen (29) investigated the flow associated with uniform tangential injection with strong circulation and a sink on the axis with a radius smaller than that of the container. The theory is developed by considering a linearized solution about weak circulation and another about strong circulation.

A particular example is discussed in which the swirling flow is generated by a rotating porous container. The linearized theory for strong circulation with weak axial flow is used. It is also assumed that the Reynolds number associated with rotation is so large that the principal

variation of the axial velocity occurs in the end wall of the boundary layer, while the radial variation occurs in the cylinder wall boundary layer. Lewellen showed the large swirl forces of the flow to be essentially two-dimensional except in a region near the boundary layers where the principle variation in the velocities occur.

4. VISCOUS BOUNDARY LAYERS IN VORTEX FLOWS

4.1 Introduction

In the previous section, theories were presented which may be applicable to the flow inside the chamber of an internal-burning rocket motor. Even though viscous effects were in general included, the interaction of the primary flow with the end wall of the container were not considered. The purpose of this section is to present some of the considerations pertinent to viscous boundary layers around rotating disks and in nozzles. The bulk of this theory is applicable for incompressible, laminar flow only. However, some considerations are given to turbulent effects.

4.2 Boundary Layers in Nozzles

The analyses presented in this section are characterized by an irrotational core of an incompressible fluid which is surrounded by a boundary layer formed at the stationary walls of a conical nozzle. In 1940, Taylor (30) presented an analysis of the swirl atomizer. This device had been studied previously by many authors. However, Taylor introduced the concept of an irrotational core surrounded by a viscous layer attached to the stationary nozzle walls. Based upon measurements of the discharge coefficients of swirling nozzle flows, he concluded that the boundary layer could occupy a significant portion of the nozzle flow area. Thus he concluded that the treatment of the swirl atomixer

by perfect fluid theory was not accurate. A schematic of the swirl atomizer and the model for the analysis of the boundary layer in nozzles with swirling flow is presented in Fig. 9.

4.2.1 Theory of Taylor

Later in 1945, Taylor (31) presented a more complete analysis of the boundary layer phenonema in the nozzle of a swirl atomizer. The following list of assumptions are common to this analysis and succeeding analyses.

1. The boundary layer is thin.
2. The pressure variation normal to the boundary layer is small.
3. There is an irrotational core which imposes its pressure on the boundary layer.
4. Terms involving radial velocity squared are neglected with respect to tangential velocity squared.

The problem Taylor chose to solve was that where the axial velocity of the core could be considered negligible. Taylor used the following velocity profiles.

$$w = \frac{\Omega E}{Rsm\alpha} f(\eta) \; ; \qquad f(\eta) = (\eta - 2\eta^2 + \eta^3) \tag{4.1}$$

$$v = \frac{\Omega}{Rsm\alpha} \phi(\eta) \; ; \qquad \phi(\eta) = (2\eta - \eta^2) \tag{4.2}$$

$$\eta = \frac{R(\alpha-\theta)}{\delta} \tag{4.3}$$

δ = The boundary layer thickness

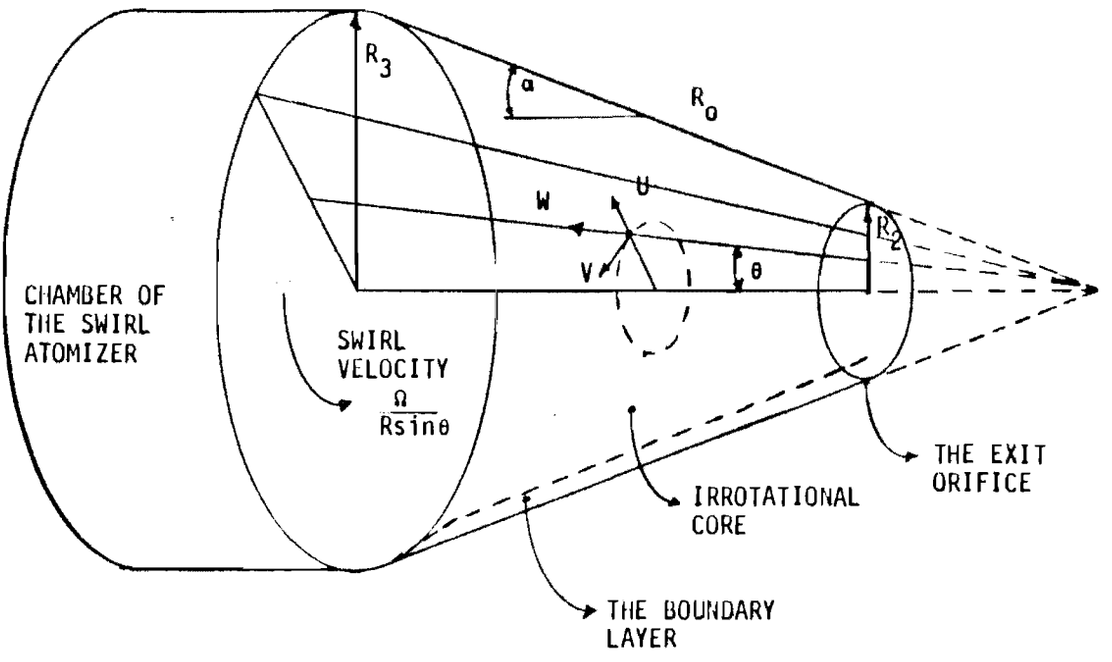

FIGURE 9 THE BOUNDARY LAYER IN A CONVERGING NOZZLE IN SPHERICAL POLAR COORDINATES

α = The cone half angle

θ = The flow angle.

Taylor derived the equations for incompressible, viscous flow in the spherical polar coordinate system subject to the general assumptions listed above. The equations were placed in integral form. The following boundary conditions were satisfied in the intergal formulations.

$$f_1 \quad \phi = 0 \; ; \qquad \eta = 0 : \qquad f = 0, \; \phi = 1, \; \eta = 1 \qquad (4.4)$$

Taylor was then able to determine the growth of the boundary layer and the direction of the flow at the nozzle surface. In conclusion, two examples were presented for a cone half-angle of 45°. When the injection velocity was 45 meters per second and the chamber pressure was ten atmospheres, the boundary layer thickness was 11 per cent of the total radius of the throat. When the chamber pressure was one atmosphere, the boundary layer was fully developed and occupies the entire flow area. A plot of the variation of the boundary layer thickness with respect to the reduced nozzle radius, R/R_o, is presented in Fig. 10.

4.2.2 Theory of Binnie and Harris

In 1950, Binnie and Harris (32) published an analysis of the swirl atomizer. In this paper, some of the general theory of irrotational, incompressible vortices was discussed. They also presented an analysis of the boundary layer growth in the nozzle. The assumptions employed were essentially those used by Taylor except that the axial velocity in the core was not necessarily considered to be neglegibly small.

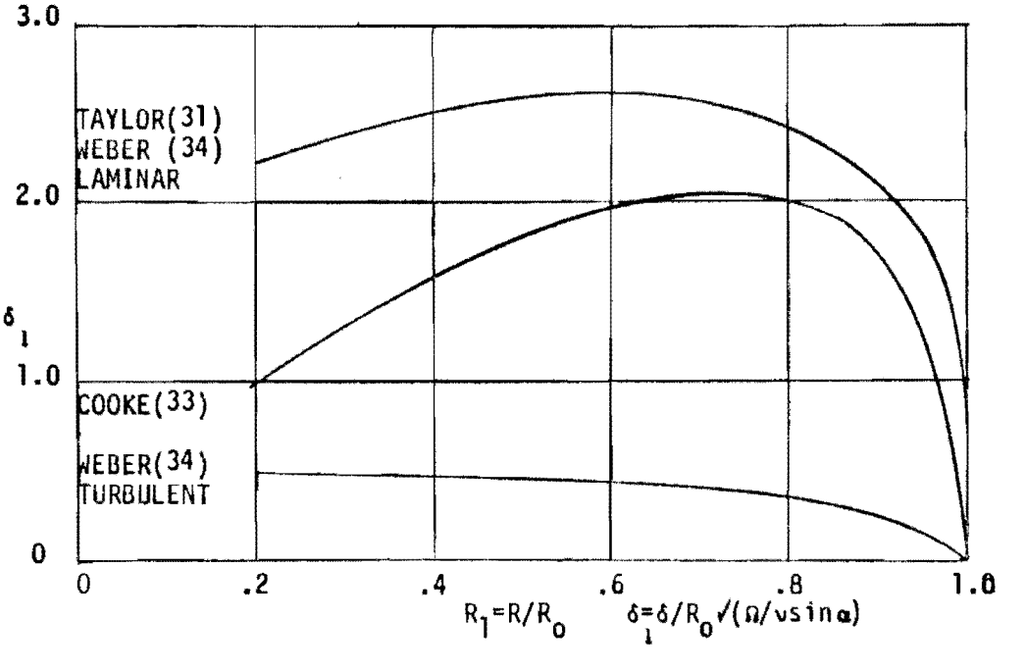

COMPARISON OF THE VARIOUS BOUNDARY LAYER THEORY FOR THE SWIRL ATOMIZER

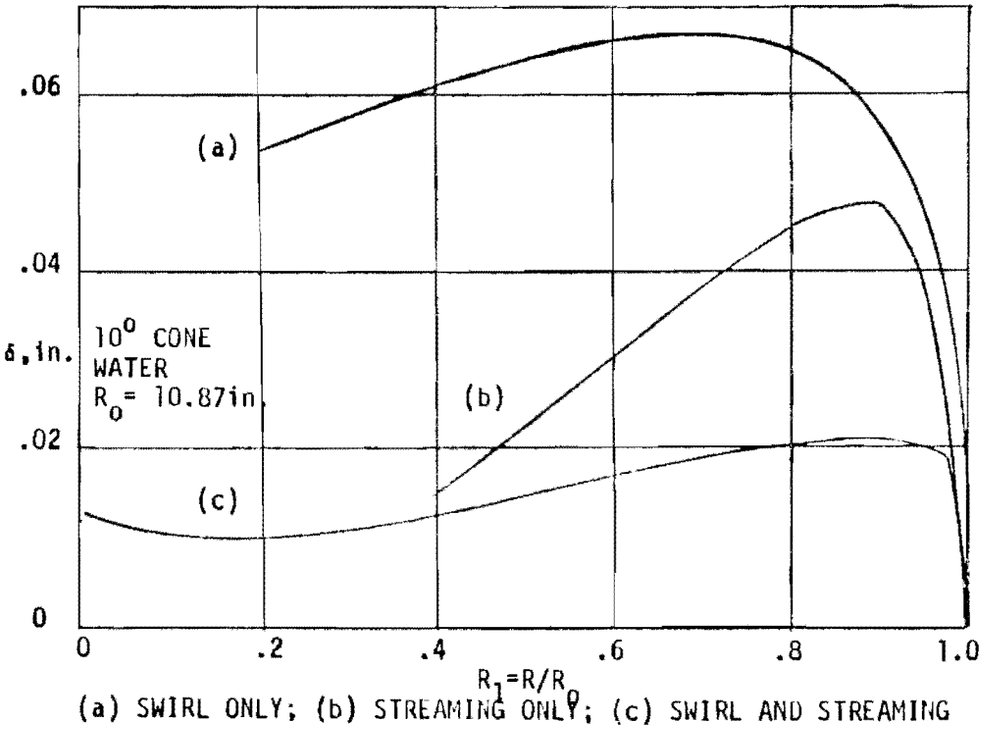

(a) SWIRL ONLY; (b) STREAMING ONLY; (c) SWIRL AND STREAMING
RESULTS OF A SAMPLE CALCULATION BY BINNIE AND HARRIS (32) .

FIGURE 10 SOME RESULTS FOR THE BOUNDARY THEORY IN CONICAL NOZZLES

By assuming the following velocity profiles, an estimate was obtained for the boundary layer thickness, δ, as a function of the distance in the nozzle.

$$W = G(R)\ \phi(\eta) \qquad \phi = 2\eta - \eta^2 \tag{4.5}$$

$$V = \frac{\Omega}{R \sin\alpha}\ \phi(\eta) \qquad \eta = \frac{R(\alpha-\theta)}{\delta} \tag{4.6}$$

δ = The boundary layer thickness (4.7)

α = The cone half angle

θ = The flow angle

In conclusion, Binnie and Harris found two simultaneous differential equations involving the pressure and velocity profiles. These equations were integrated using a forward marching numerical method and assuming contant coefficients over small steps. The results of their calculations were compared to Taylor's analysis (31) which was based upon zero actual velocity in the core. Binnie and Harris found that the result for the boundary layer thickness is of the order of one-third to one-fifth of Taylors' boundary layer thickness as shown in Fig. 10.

4.2.3 Theory of Cooke

In 1951, Cooke (33) published an article concerning the boundary layer buildup of Taylor's problem (31) wherein the axial velocity of the core was assumed to be negligible. The main purpose of this article was to show that the boundary layer thickness associated with the axial velocity was not necessarily the same as the boundary layer thinkness associated with

the swirling component. In other words, he postulated that two boundary layer thicknesses are required.

$$W/W_o = .995 \quad \text{- defines the location of } \delta$$
$$V/V_o = .995 \quad \text{- defines the location of } \Delta \tag{4.8}$$

Cooke incorporated the boundary layer conditions used by Taylor, allowing an additional set of boundary conditions for Δ.

$$W = 0 \qquad V = 0$$
$$\frac{\partial^2 W}{\partial \theta^2} = r/\nu \; R \sin\alpha \qquad \text{at } \theta = \alpha \tag{4.9}$$
$$\frac{\partial^2 V}{\partial \theta^2} = 0$$
$$W = 0, \; \partial\omega/\partial\theta = 0 \qquad \text{at } \theta = \alpha - \delta/R$$
$$V = \frac{\Omega}{\sin\alpha}, \quad \frac{\partial \omega}{\partial \theta} = 0 \quad \text{at } \theta = \alpha - \Delta/R$$

The solution for the boundary layer thicknesses then preceeded in the manner of Pohlhausen by assuming polynomials for the velocity profiles through the boundary layer. Cooke found that the boundary layer thickness determined in this manner was approximately one-half that of Taylor's problem, and therefore, between the analyses of Taylor (31) and Binnie and Harris (32), as shown in Fig. 10.

4.2.4 Theory of Weber

In 1956, Weber (34) presented an analysis of the boundary layer in a conical nozzle. Once again, the boundary conditions of Taylor's problem

were assumed. However, in this paper, the Pohlhausen intergal technique was used for both laminar and turbulent flows. For the laminar case, the results are identical to Taylor's results because the same velocity profiles and boundary conditions were assumed.

In the turbulent case, the one-seventh power law for the turbulent boundary layer was used for the tangential velocity distribution.

$$V = V_{\delta}\, \eta^{1/7} \tag{4.10}$$

Then, due to a lack of data, Weber assumed the axial velocity to be

$$W = W_{\delta}\, E\, (\eta^{1/7} - \eta) \tag{4.11}$$

so that the boundary conditions of zero velocities could be satisfied at the wall. The assumption of this type of velocity profile makes it impossible to determine the wall stresses since the gradients become infinite at the wall. Therefore an experimentally obtained correlation was used for the wall shear stress.

$$\tau\omega = 0.0225\, \rho\, V^{7}\, (\nu/y)^{1/4} \tag{4.12}$$

The stress components at the wall were determined next and substituted together with the assumed velocity profiles into the momentum integral equations. The resulting boundary layer thickness was found to be approximately one-fourth that of Taylor's laminar case, as shown in Fig. 10.

4.2.5 Conclusions

In conclusion, it appears that the theory for the development of the boundary layer in a simple conical nozzle for incompressible flow is not

well understood. However, the boundary layer does seem to occupy a portion of the nozzle which can be large when the chamber pressures are small and the axial velocities are small. In a rotating rocket motor, the walls of the motor would be rotating in direct proportion to their radial position. The effect of moving walls would be to reduce the velocity difference between the core and the walls, thereby reducing the boundary layer buildup.

4.3 Boundary Layers Near Rotating Disks

This section deals with a class of problems associated with the flow of a viscous fluid bounded by rotating disks. T. Von Kármán (35) first attacked this problem in 1921. He obtained a solution for a steady, viscous flow in a semi-infinite region bounded by a rotating place. The solution was exact in that no assumed velocity profiles were required. However, the resulting differential equations required numerical solution.

4.3.1 Theory of Batchelor

In 1950, Batchelor (36) extended Von Kármán's analysis to include a flow bounded by two infinite rotating disks. In general, two classes of problems were studied: one, in which the plates rotated in the same direction, and the second, in which the plates rotated in the opposite sense. Batchelor worked out these solutions qualitatively to illustrate the pertinent features of the flow.

Batchelor began with the equations of steady, viscous, incompressible, axisymmetric flow. The only restriction placed upon the equations was the assumption that the velocity of the fluid flowing normal to the disk was a function of axial position only.

$$W = W(z) \tag{4.13}$$

The boundary conditions are those of zero velocities relative to the rotating plates

$$\begin{aligned} w = u = 0 \; ; \quad v = \omega r \quad \text{at } z = 0 \\ w = u = 0 \; ; \quad v = \gamma_1 r \quad \text{at } z = d \end{aligned} \tag{4.14}$$

where

ω = angular velocity of the first disk

γ = angular velocity of the second disk

or, γ_1 = angular velocity of the fluid far from the first disk

Solutions were obtained for one and two disk systems as a function of γ_1/ω. The results of these studies are presented in Fig. 11.

4.3.2 Theory of Rodgers and Lance

In 1949, Rodgers and Lance (37) presented additional studies of a rotationally symmetric flow of a viscous fluid in the presence of an infinite rotating disk. In their analysis, Rodgers and Lance treated the following cases employing similarity profiles.

1. The fluid and the disk rotating in the same sense
2. The fluid and the disk rotating in the opposite sense
3. The fluid rotating as a solid body at infinity.

The particular property profile functions employed are given below.

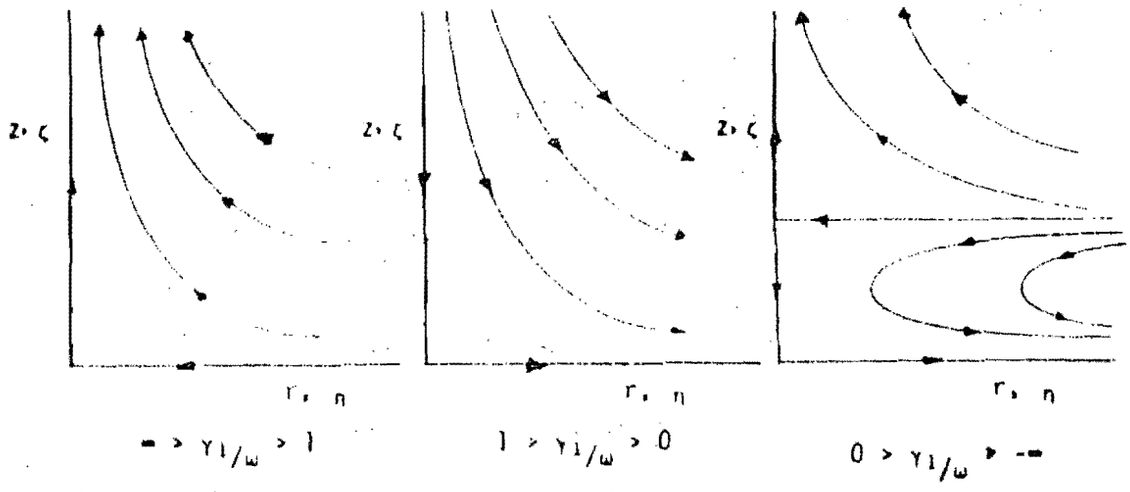

FLOW PATTERNS FOR A SINGLE DISK

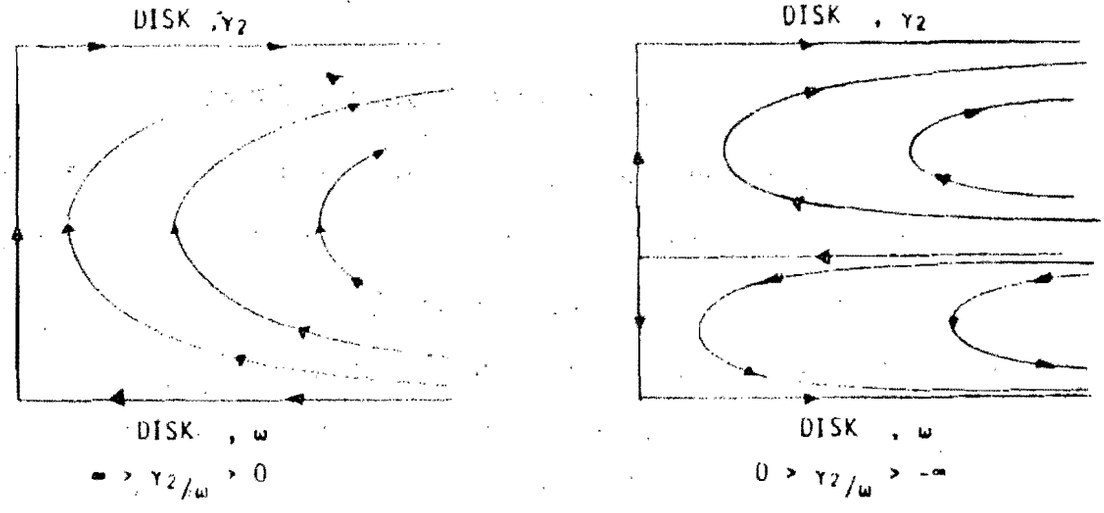

FLOW PATTERN FOR TWO ROTATING DISKS

FIGURE 11 THE FLOW PATTERNS BETWEEN DISKS DUE TO BATCHELOR (36).
(Taken from reference (36) , Batchelor)

$$u = r\,\Omega\,F(\zeta)$$

$$v = r\,\Omega\,G(\zeta)$$

$$w = (\nu\Omega)^{1/2}\,H(\zeta) \qquad (4.15)$$

$$P/\zeta = \nu\Omega\,P_0(\zeta) + 1/2\;k\;\Omega^2\;r^2$$

$\Omega \equiv$ The angular velocity of the disk

These equations were then introduced into the Navier-Stokes equations yielding a set of four ordinary differential equations.

Physically acceptable solutions to these equations were found for all values of the ratio of fluid angular velocity at infinity to the disk angular velocity for case 1 described above. In each instance, the boundary layer was attached to the disk and the motion approached solid body rotation in the fluid far from the disk.

In case 2, where the fluid is rotating in the opposite sense as the disk, there existed regions of unsteady solutions only. The only correction for such cases was the application of suction to prevent the boundary layer leaving the disk. It was concluded that when the flow along the disk was radially inward, the similiarity solution employed may not be valid, especially if separation is likely to occur.

4.3.3 Theory of Mack

In a series of reports by Mach (38, 39), the problem of the interaction of a primary vortex field with a stationary disk was studied. It had been shown previously by experiment that the presence of the end walls cause a

radial in-flow due to the imbalanced radial pressure gradient in the boundary layer. It was the purpose of Mack's reports to investigate methods of analytically predicting the amount of in-flow and its effect upon the primary stream in the chamber.

Various techniques were employed to obtain solutions for the incompressible, boundary layer equations on a disk. The method of Von Kármán was employed initially, however, Taylors' (31) and Cooke's (33) methods were also applied. Stewartson velocity profiles were used in these integral techniques and these results were compared to a set of eleven pairs of velocity profiles. The Stewartson profiles are very useful in this respect since they allow exact solutions of the boundary layer equations at the edge of the disk.

To complete the study primary flow field tangential velocities of the following form were assumed.

$$V \alpha 1/r^n$$

$$-1 < n < 1$$

These were employed to obtain certain boundary conditions for the boundary layer. In the case of $n = +1$, or a free vortex, the radial mass flow increase monotomically with decreasing radius. For $n \neq 1$, the radial mass flow reaches a maximum at some radius less than the centerline. When $n = -1$, a solid body vortex, the radial mass flow is only 30% of the free vortex case and its maximum value occurs at $r/r_o = .74$.

4.3.4 Theory of King and Lewellen

King and Lewellen (40, 41, 42) have prepared a number of reports on the action of the viscous boundary layer associated with the end walls of

a vessel containing a vortex flow. These studies were made because it had been found experimentally that these end-wall boundary layers significantly affect the flow in the chamber. Previous studies of vortices in chambers are strickly applicable for infinite cylinders only since boundary layers on the end walls were neglected. It should be noted that these solutions are limited to stationary end walls.

The calculations were performed numerically employing several variations of the classical Kármán- Pohlhausen integral technique for incompressible flows. The tangential velocity of the main stream was varied by assuming,

$$V \alpha r^{n}$$

where,

$$-1 < n < +1$$

The value of the exponent n was varied parametrically. It was found that the most drastic effects upon the main stream occurred when n = -1. Since the end wall was a stationary boundary, the tangential velocity of the free stream is retarded as it approaches the wall, thus losing centrifugal force. When n = - 1, the primary stream was a free vortex, and the pressure gradient associated with a free vortex is imposed upon the wall. The result was an unbalanced pressure gradient at the wall. Thus, an inward flowing radial flow was generated, associated with the unbalanced radial pressure gradient. Continuity required the presence of an axial velocity in the presence of the induced radial velocity. Thus, secondary flows are set up in the main chamber. In addition, the boundary layer was able to control a great deal of the total mass flow rate.

The results of the studies performed are compared to the theories of Cooke (33), Taylor (31), Weber (34), and Mack (38). It is found that when $n \neq -1$, the results of all the analyses were approximately the same. However, when $n = -1$, considerable discrepancies in the values of the radial inflow were found.

4.3.5 Theory of Rosenweig, Lewellen, and Ross

In a paper published in late 1964, Rosenweig, Lewellen, and Ross (43) presented an analysis of a contained vortex in which fluid is injected tangentially through porous, rotating walls. This paper differs from those published previously by Lewellen (27, 28) in that the flow field is divided into three fundamental regions. A schematic of the physical model is presented in Fig. 12.

Region I consists of the primary flow region which is free from edge effects and boundary layer interaction. It occupies a volume defined by the tank walls, the end-wall boundary layer, and the drain opening. Region II consists of the boundary layer associated with the end walls. Region III is bounded by an imaginary cylinder extending up from the drain opening. Each of these regions is considered to be viscous in nature. However, in Region II, axial gradients predominate, whereas in Region II and III, the radial gradients predominate.

Approximate solutions are employed in each of these regions. A complete flow field is built up by prescribing suitable matching conditions between these regions. The solution is based upon the assumption of large circulation and small axial velocities.

The approximate boundary layer solution of Rott (44) is used along the end-walls and is matched to the solution of the primary flow field. The authors specify the stream function distribution in the central core, region III. A provision is made, however, to allow for the injection of fluid from the end-wall boundary layer into the drain opening. The equations apply to an incompressible, laminar flow field where appropriate boundary layer assumptions are made in Regions II and III. The solutions are parameterized in terms of

R_{er} = the radial Reynolds number

r_e/r_o = the ratio of drain opening to the cylinder radius

ξ = the dimensionless axial coordinate

$A = \frac{-.26}{(R_{et})^{1/5}} \frac{\Gamma_o r_o}{P_o l}$ = the end-wall boundary layer interaction term.

where,

r_o = the cylinder radius

$\Gamma_o = r_o^2 \omega$

l = the length of the cylinder

Q_o = the volume flow rate

R_{et} = the tangential Reynolds number

Solutions are presented in terms of the ratio, Γ/Γ_o, the ratio of the point circulation to the wall circulation, as a function of the reduced radial coordinate, r/r_o. The solutions are computed for constant values of the above parameters. However, only $r_e/r_o = 1/6$ is used. It is found

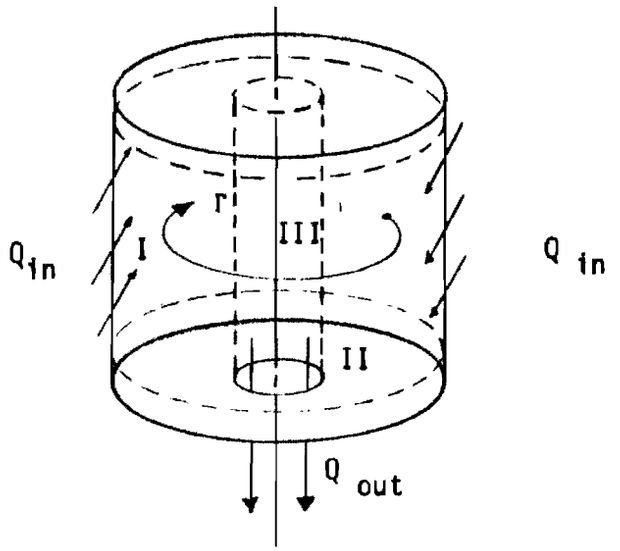

FIGURE 12 A SCHEMATIC DIAGRAM FOR THE THEORY OF ROSENZWEIG et al (43).

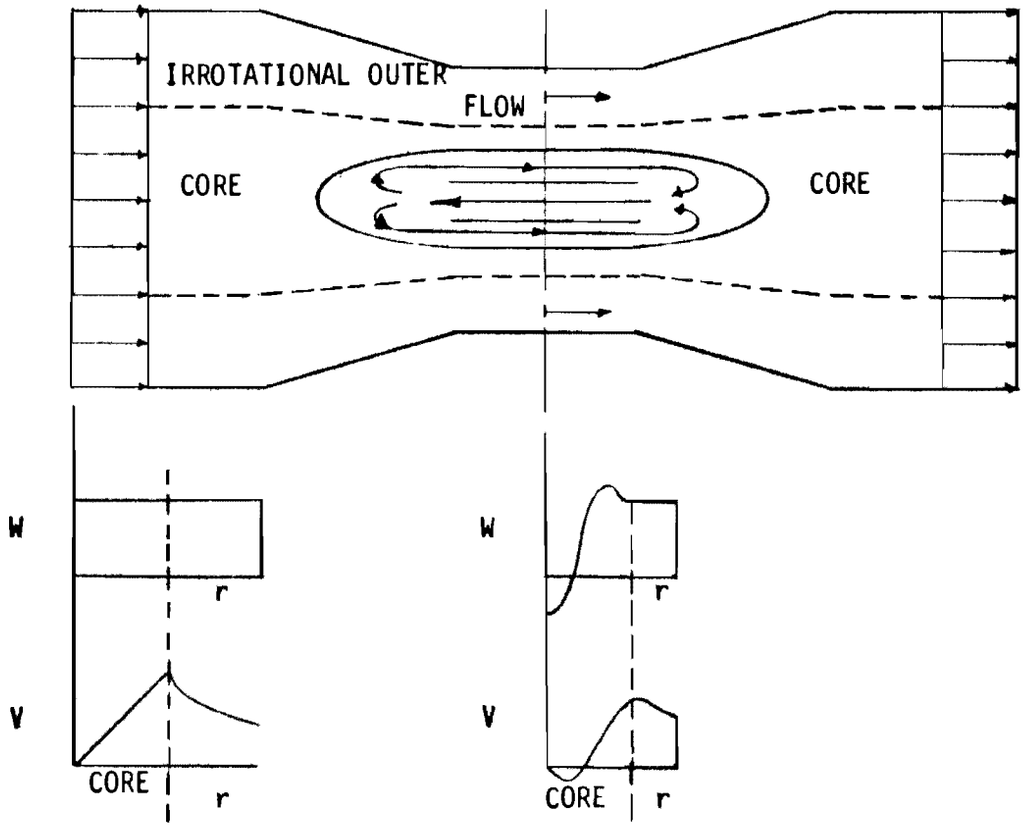

FIGURE 13 SOME RESULTS OF THE THEORY OF BURGERS (53) AND WESKE (52) .
(Taken from reference (52) , Weske)

that when $A \leq 1$, the boundary layer interaction is not large. The above is also true when R_{er} is small, regardless of the magnitude of A. The axial variation of r/r_o with ξ is small in these cases. However, when A and, or, R_{er} are large, the boundary layer interaction is felt throughout the entire flow field. Also, the effects of mass ejection from the boundary layer tends to increase until reverse flow and recirculation are necessary to keep the boundary layer supplied with fluid.

4.3.6 Theory of Rott and Lewellen

A comprehensive review of the phenomena of boundary layer interaction with a vortex flow field is presented by Rott and Lewellen (45). In this work, the theories for both rotating and stationary disks are discussed. In addition to the review of past research, Rott and Lewellen propose an analytic method for predicting the thickness of the boundary layer and the role of mass ejection for the case of a turbulent boundary layer and a laminar flow field.

The theory is developed by assumming universal, turbulent, boundary layer velocity profiles. The simplicity of the method makes it useful for rapid estimates of boundary layer effects on the end-walls of a rotating container. As in other previous works in the field, the velocity of the main flow field is assumed to vary in the following manner.

$$V = c\, r^n$$

$$-1 < n < +1$$

The results of this theory are presented in Fig. 12. It may be noted that when a free vortex exists, the radial inflow can be quite large, whereas when $n \neq -1$, a maximum exists. These results are in agreement with Mack (38, 39), King and Lewellen (40, 41, 42). However, these results differ from the results of Cooke (33). This is attributed to the use of a two parameter boundary layer by Cooke.

5. BACKFLOWS AND VORTEX BREAKDOWN

5.1 Introduction

The phenomenon of backflow or reversed axial flow in a vortex has been a topic of interest for some years. A classical example of backflow is found in the Ranque-Hilsch vortex tube. In this case, gases are injected tangentially into an open-ended tube. A hot gas, rotating in one direction, is found at one end, while a cold gas, rotating in the opposite sense, is found at the other end. This effect has been noted in a number of experiments and is analytically predicted with the models of Sullivan (22) and Donaldson and Sullivan (16, 17, 18).

Aside from straight tube flows, backflows have been noted in diverging and converging sections for both initially solid and free vortices. As yet, the analytical description of the process is incomplete and considerable controversy exists as to the role of viscosity in setting up and maintaining the reverse flow. In many cases, such as the vortex tube, it seems that the reverse flow is predominantly a viscous effect. There are indications, however, that the concept of vortex breakdown in which a small stagnation region of locally reversed flow near the axis exists, is primarily due to dynamic instability. This action is triggered by some small change in the boundary conditions so that the flow must readjust.

In this section, the concepts of vortex breakdown and backflows will be discussed. There are numerous references to this phenomena. However,

only a few of these will be presented. Lord Rayleigh (46, 47, 48) and Lord Kelvin (49) wrote about the conditions of stability of fluids in a vortex flow in the later parts of the 19th century. The primary conclusion of these studies is, that to posses dynamic stability in the presence of infinitesimal disturbances, the flow must have a circulation which constantly increases with radius. In addition, the circulation should posses the same sign along a radius. When this is not the case, instabilities will be developed, as in the well known case of rotating coencentric cylinders. This concept has recently been expanded by Ludweig (50) who considers the stability of an inviscid, spiralling flow in a narrow cylindrical amnulus. This study is a direct extension of Rayleigh's work which allows radial gradients to exist in the axial velocity. By employing small disturbance theory, the stability boundary is deduced. It is shown that very small radial gradients can cause a flow which satisfies Rayleigh's criterion to go unstable. The work of Ludwieg has been extended by Kiessling (51) to include viscous effects for a flow between rotating cylinders of small separation.

5.2 Theory of Burgers and Weske

In two articles prepared at the University of Maryland, Weske (52) and Burgers (53) investigated the existence of backflow as derived from "stretching" a rotational vortex core in converging or diverging passages as shown in Fig. 13. The analyses presented are for a solid-body vortex core surrounded by an irrotational vortex which flows from a section of uniform radius to another section of a different radius. The equations for the flow are derived from an incompressible, inviscid, vortex flow in

a cylindrical coordinate system.

Weske first investigated the problem in general terms. However, Burgers expanded the analysis and presented particular solutions. Burgers found that it was possible to achieve exact solutions for the case of a core with solid-body rotation and initially uniform axial velocity profiles surrounded by an irrotational vortex. The solution was derived from classical incompressible fluid mechanics by considering the following set of equations.

LAMB'S EQUATION

$$\nabla(P/\rho + 1/2\ q^2) = \bar{q} \times \bar{\omega} \tag{5.1}$$

where,

$$\bar{\omega} = \nabla \times \bar{q} \quad \text{The vorticity vector} \tag{5.2}$$

CONTINUITY EQUATION

$$w = \frac{1}{2\pi r}\ \frac{\partial \psi}{\partial r}\ , \qquad u = \frac{-1}{2\pi r}\ \frac{\partial \psi}{\partial r} \tag{5.3}$$

INITIAL CONDITIONS

$$w = W\ , \qquad v = r\ \omega_o. \tag{5.4}$$

By conserving angular momentum along streamlines which flow from one section of zero radial velocity to another, the following equation was derived.

$$\frac{d^2 w_2}{dr_2^2} + \frac{1}{r^2}\ \frac{dw_2}{dr_2} + \frac{4\ \omega_o}{W}\ (w_2 - W) \tag{5.5}$$

This equation has a Bessel function solution,

$$w_2 = W(1 - a J_0 (\frac{2 \omega_0 r_2}{W})) \tag{5.6}$$

where,

W = the axial velocity at the inlet

ω_0 = the angular velocity at the inlet

r_2 = the radial coordinate at the second straight section

The constant, a, is an undetermined coefficient which can be evaluated from conservation of mass considerations.

$$2\pi \int w_2 r_2 dr_2 = \pi(r_2^2 + a \frac{W r_2}{\omega_0} J_1 (\frac{2\omega_0 r_2}{W})) \tag{5.7}$$

$$1 + \frac{aW}{\omega R^*_2} J_1 (\frac{2\omega R^*_2}{W}) = (\frac{R^*}{R^*_2})^2 \tag{5.8}$$

where,

R^* = the inlet radius of the rotational core

R^*_2 = final radius of the core

For the case where the rotational core extends throughout the flow field, the results are particularly simple.

$$a = \frac{1-n^2}{n^2} \frac{n\alpha}{2 J_1 (n\alpha)} \tag{5.9}$$

$$w_2 = W(1 + \frac{(1-n^2)}{n^2} (\frac{n\alpha}{2 J_1 (n\alpha)}) J_0 (\frac{2\omega_0 r_2}{W}) \tag{5.10}$$

where,

$n = R_2/R$

$\alpha = 2\omega_0 R/W$

Thus, it can be seen that negative axial velocities can occur under a number of conditions.

$$\begin{aligned} &1.\ n^2 > 1 \\ &2.\ J_0 < 0\ , \quad J_1 > 0 \\ &3.\ J_1 < 0\ , \quad J_1 > 0 \end{aligned} \tag{5.11}$$

For the case of converging flows, n is less than one. However, J_0 and J_1 may be negative depending upon their arguments. For diverging flows, $n > 1$. Backflow can be expected provided the Bessel functions remain positive. In addition, it is pertinent to add that no negative velocities actually occur unless the above criteria cause negative terms which are larger than the initial axial velocity, W. It is also interesting to note that multiple regions of back flow can be obtained by proper choice of the arguments of the Bessel functions. However, these become successively smaller and finally become smaller than the initial axial velocity term.

The more general case of the rotational core surrounded by the irrotational vortex is also treated in some detail by looking at limiting cases. One of the more interesting cases occurs for continuous flow with no radius change. In this case, the Bessel function solution is appropriate for radial equilibrium, however, not necessarily stable equilibrium. The question of instability is studied by perturbing the Euler equations. It is found that the perturbed equations allow undamped oscillations to occur.

5.3 Theories of Squire, Brooke, Benjamin and Lambourne

In 1960, Squire (54) proposed a mechanism for the vortex breakdown phenomenon. It was postulated that when the flow could sustain infinitesimal standing waves, a characteristic bubble would form along the axis, the idea being that waves generated downstream, or at the exit, would collect at the critical point. However, it was later pointed out by Benjamin (55) that the group velocity of such waves would allow only upstream disturbances to be felt at the critical point.

In 1962, Benjamin (55) published his theory of the vortex breakdown phenomena which was closely related to the experimental work of Harvey (56). Harvey had described the formation of stagnation regions of locally reversed flow on the center line of a vortex tube. The theory of Benjamin closely parallels the concept of the hydraulic jump problem where a flow in a channel can exist in two conjugate pairs, namely supercritical and subcritical. The definition of the critical condition is that condition when the velocity of the long waves of water is the same as the axial velocity of the flow (Froude number = 1.0). Benjamin hypothesized that an analogous condition exists in swirling flow such that there can be a sudden transition from the supercritical to the subcritical condition.

The theory is postulated employing the calculus of variations to establish the concept of conjugate flows based upon a deficiency of the "force flow", S.

$$S = \int_0^r (\rho w^2 + p)dA$$

Associated with the conjugate pair of flows is a gain of force flow when the transition from supercritical to subcritical occurs. Benjamin further investigated the conditions for the onset of transition which occurs when the ratio of axial to tangential velocity is of the order of 1.

A subsequent publication by Benjamin (57) was presented in 1964. In this paper, the essential ideas of conjugate flows in an incompressible swirling flow are reaffirmed. In 1965, Lambourne (58) published an analysis of vortex breakdown phenomena. The theory of this work closely parallels those of Weske (52), Burgers (53), and Benjamin (55). In this paper conditions for the critical conditions are derived in a somewhat different fashion. However, the result is the same as that found by Squire (54) and Benjamin (55). The analysis proceeds upon the basis of the Bessel function solution of Burgers (53). In this study, various changes were made in the external flow and regions of no apparent solution were found, thus suggesting a finite transition or vortex breakdown.

5.4 Theory of Gore and Ranz

In 1964, Gore and Ranz (59) presented a paper illustrating backflow occurring in divergent sections of a flow generated by a rotating porous plate. A theory was developed employing successive approximations to a set of simplified Navier-Stokes equations. Once again the condition of back-flow occurred when the ratio of the axial velocity to the tangential velocity at the wall was of the order of one. Regions of back-flow were predicted, which were preceeded by a stagnation point. This phenomenon

has direct application to the flame pattern of a swirling flow combustor.

5.5 Conclusions

In conclusion, the existence of backflow due to vortex breakdown has been analytically and experimentally verified. The theory, however, is still qualitative since the phenomenon is related to the stability of the flow. The characteristic axisymmetric bubble of reverse flow occurs most frequently in the diverging section of a supercritical flow. The analytical and experimental work of Burgers (53) and Weske (52) indicate that the phenomenon may also occur in a converging section.

6. BURNING RATE AUGMENTATION IN AN ACCELERATION ENVIRONMENT

6.1 Introduction

The rotation imparted to a solid propellant rocket motor not only changes the flow of the gases, but also affects the burning rate of the propellant. The variations in burning rate have been studied most extensively by experimental methods and are reported upon in Ref. 69. However, recently a few analytical investigations in this field have been attempted with varying success.

6.2 Theory of Glick

Glick (60) advanced a theory to account for the effect of acceleration forces on the burning mechanism of solid propellants. This was accomplished by extending the grannular diffusion model of Summerfield (61) for the burning of composite solid propellants at high pressures. Since Summerfield's analysis is qualitative and empirical in nature, the extension to account for acceleration effects should also be viewed in the same manner.

Two basic effects are considered with respect to acceleration fields.

1. Pressure gradients across the gas phase reaction zone.
2. Differential forces acting upon particles of different density.

The first possible effect was eliminated by an order of magnitude analysis. It was shown for an acceleration field of 50,000 g's and a mean chamber pressure of 600 psia, that the pressure gradient across the reaction zone was less than .01%. Therefore, only the effect of the acceleration

field acting upon the density inhomogenities was incorporated into the analysis. There can be two main sources of density inhomogenities.

1. The heterogeneous nature of the reaction zone.
2. The mean temperature gradient through the reaction zone.

The effect of these density inhomogenities due to the acceleration forces acting normal and parallel to the propellant surface were investigated. It was concluded, by considering the theory of free convection flow for the case of normal accelerations and boundary layer flow for the case of parallel accelerations, that the mean temperature gradient has only secondary effect.

Thus, the effect of acceleration forces is primarily concerned with the density inhomogenities produced by the pockets of fuel vapor imbedded in a homogeneous oxidizer vapor. In the high pressure limit, the granular diffusion model is primarily concerned with thickness of the gas phase reaction zone.

$$\delta_r'' = V_{fv}\, T_{fv} \tag{6.1}$$

where

δ_r'' = thickness of the gas phase reaction zone

V_{fv} = normal velocity of the fuel vapor

T_{fv} = lifetime of the fuel vapor pocket.

Since the burning rate is assumed to be inversely proportional to the thickness of the gas phase reaction zone, the effects of acceleration on burning should be explainable in terms of accelerations effects upon V_{fv} and T_{fv}, since any relative motion between the fuel pocket and the oxidizer vapor will increase the interdiffusion rate. In addition, the flow of the oxidizer

vapors can be reduced if the acceleration is into the propellant. Thus, two effects can be postulated: a scalar effect causing an increase in interdiffusion which is independent of the direction of the acceleration field, and a vector effect which can increase or decrease the thickness of the gas phase reaction zone.

Based upon these considerations, Glick proposed a model allowing for both a vector contribution and a scalar contribution to the burning rate. The final burning rate equation was written in terms of the Reynolds number, the Grashof number, the Schmidt number, and the diameter of the fuel vapor pocket.

It was concluded that some of the characteristics noted in experimental observations could be predicted. However, the analysis failed at high accelerations, since the model predicts that burning rate increased without bound with increasing acceleration whereas experimental results indicated a maximum burning rate with g level.

6.2.2 Conclusions from Glick's Theory

1. "The effects of acceleration induced pressure difference across the mean flow of the gas phase reaction zone on the burning rate of nonmetallized composite propellants are negligible."
2. "The major effect of accelerations on the burning rate of a nonmetallized composite solid propellant is derived from the effect of acceleration on the heterogeneous nature of the gas phase reaction zone."

3. "The granular diffusion flame model correctly predicts the trends for the variation of the burning rate of a nonmetallized composite propellant with respect to the direction of the acceleration vector relative to the burning surface."
4. "The granular diffusion flame model correctly lead to an upper bound on burning rate changes when the acceleration vector is normal to and into the burning surface."
5. "The ratio of the burning rate of a nonmetallized composite propellant in an acceleration field to its static value is not dependent upon either catalyst content or initial temperature when the acceleration vector is parallel to the burning surface."
6. "The ratio of the burning rate of a nonmetallized composite propellant in an acceleration field to its static value is generally reduced by the following:"
    a. Addition of burning rate catalysts.
    b. Reduction of the mean diameter of the oxidizer particles.
    c. Increasing the initial temperature of the propellant.
7. "The burning rate of a nonmetallized composite propellant in an acceleration field when the thickness of the gas phase reaction zone is much greater than the diameter of a pocket of fuel vapor is given by

$$\frac{r}{r_o} = C_1 \frac{G_{rd}^{1/2} \cos\theta}{C_d \, 1/2 \, Re_o} + \left[C_1^2 \frac{G_{rd} \cos^2\theta}{C_d \, Re_o^2} + \frac{Sh}{Sh_o} \right]^{1/2} \qquad (6.2)$$

where,

Sh = the Sherwood number - $h_o \, d_{fv}/Dg$

$G_r = a \cdot \Delta\rho \; d_{fv}^3/\mu g^2$ = The Groshoff number

Re = the Reynolds number = $\rho \; p \; r_o \; d_{fv}/\mu g$

$C_{1,2}$ = constants to be determined from experiment

o = zero acceleration

a = acceleration

C_D = the drag coefficient for the particle

θ = the angle of the acceleration vector to the propellant surface.

6.3 Theory of Crowe et al

In a final report for a contract related to the study of spin stabilized rocket motors, Crowe et al. (62) discussed various models for burning rate augmentation due to motor rotation. These are:

1. Effect of a centribugal force field on the gas flow from a solid propellant burning surface.
2. Contribution of particle combustion zone to surface heating.
3. Retention of metal oxide particles on the burning surface.

6.3.1 The Effect of a Centrifugal Force Field on the Gas Flow from a Solid Propellant

When the pressure gradient was small, the momentum and energy equations for the gas flow at the propellant surface in an acceleration field are given by,

$$u \frac{du}{dx} = - \alpha = \text{centrifugal acceleration term} \qquad (6.3)$$

$$\rho u \frac{dh_o}{dx} = \rho u_\alpha + \frac{d}{dx}\left(\frac{k}{C_p}\frac{dh}{dx}\right) + \rho \dot{Q} \tag{6.4}$$

where,

h_o = stagnation enthalpy

h = static enthalpy

k = thermal conductivity

C_p = specific heat at constant pressure.

By examining the following ratios, some estimate of the effect of acceleration can be obtained.

$$\frac{\alpha\delta}{u^2} \tag{6.5}$$

$$\frac{\alpha\delta}{C_p(T_f - T_s)} \tag{6.6}$$

where

δ = flame stand off distance

T_f = flame temperature

T_s = surface temperature

α = acceleration g's

when

$$\delta \leq 1 \text{ mm}$$

$$\frac{\alpha\delta}{u} = O(\alpha \cdot 10^{-4}) \tag{6.7}$$

$$\frac{\alpha\delta}{C_p(T_f - T_s)} = O(\alpha \cdot 10^{-8}) \; . \tag{6.8}$$

Thus, no significant effects of rotation should be felt until the acceleration approaches 1000 g's. Therefore, it was concluded that the acceleration field does not drastically affect the velocity and temperature fields at the propellant surface.

6.3.2 The Contribution of Particle Combustion Zone to Surface Heating

While the acceleration field does not greatly influence the velocity and thermal fields of the gases, the solid particles in the flow may be significantly affected by acceleration. When the acceleration was directed into the burning surface, the metal particles were retarded, thus enhauncing heat transfer back to the propellant surface.

The distance from the propellant surface to any particle in the flow, assuming Stokes flow, is given by,

$$S = (t - \tau - te^{-t/\tau})(u - \alpha\tau) \tag{6.9}$$

where,

t = time

$\tau = \frac{2}{g} \frac{\rho_p r_p^2}{\mu}$

μ = gas viscosity

It may be noted that when,

$$\tau = \frac{u}{\alpha} \tag{6.10}$$

the particles will remain at the surface. Thus a critical particle size can be deduced for retaining the particle at the propellant surface.

$$r_p = \left[\frac{g}{2} \frac{\rho_s \dot{r} \mu (1-w)}{\rho_p \alpha \rho_g} \right] \tag{6.11}$$

where

w = aluminum loading

$\dot{r}$ = burning rate

ρ_s = density of the propellant

In order to determine the heat transfer at the surface, the combustion zone was broken into four regions.

1. Region 1 - No heat addition to the gas; $\dot{Q} = 0$
2. Region 2 - Combustion of the gas; $\dot{Q} = \frac{\dot{m} Q_{Rg}}{\delta_2}$
3. Region 3 - Particle ignition; $\dot{Q} = 0$
4. Region 4 - Particle combustion; $\dot{Q} = \frac{\dot{m} Q_{Rp}}{\delta_4}$

where,

$\dot{Q}_{Rg}$ = heat of reaction for the gas

$\dot{Q}_{Rp}$ = heat of reaction for the particles

An energy equation is then postulated assuming the kinetic energy to be small compared to the thermal energy.

$$\frac{d^2T}{dy^2} + \frac{\dot{Q}}{k} = \frac{\dot{m} C_p}{k} \frac{dT}{dy} = \frac{1}{L} \frac{dT}{dy} \tag{6.12}$$

This equation has the following general solution,

$$T = C_2 e^{y/L} + \frac{L \dot{Q} y}{k} + C_1 \tag{6.13}$$

where C_1 and C_2 are constants of integration.

The above equation can be used for regions 2 and 4. Combining these solutions and employing the proper boundary conditions for each region, the temperature at any point can be determined as a function of position. It was concluded that, unless the solid particles are in the order of one micron or less above the surface, no appreciable additional heat transfer will occur as a result of particle combustion zone displacement.

6.3.3 The Retention of Metal Particles on the Burning Surface

Based upon the previous analyses, the effects of the acceleration field must be primarily in the retention of solid particles on the surface, since only negligible effects are found for the displacement of the gas and particle combustion zones.

The expression for a critical particle size as derived earlier can be written,

$$r_{pc} = \left(\frac{3}{10} \frac{C_D \, Re \, \mu \, u_s}{\delta_p \, \alpha}\right)^{1/2} . \tag{6.14}$$

For Stokes flow, where u_s = the gas velocity at the surface,

$$r_{pc} = \left(\frac{9}{2} \frac{u u_s}{\rho_p \alpha}\right)^{1/2} . \tag{6.15}$$

Particles larger than this size will be burned at the surface until they reach a diameter less than the critical diameter whereupon they will move into the gas stream. The increase in burning rate was a function of the additional heat released to the propellant surface as the particle burns.

The actual burning rate law was postulated as a ratio of the burning rate under rotation to that under no rotation.

$$\frac{\dot{r}_{\omega}}{\dot{r}_{\omega=0}} = \frac{1}{1 - \frac{w_m L}{h_r} H\left(\frac{r_{pc}}{r_{pm}}, \sigma, \frac{t}{t_{pm}}\right)} \qquad (6.16)$$

where,

H = a function to be determined

h_r = the heat of vaporization of the particles

w_m = the propellant metal loading weight fraction

L = the heat transfered per unit mass of particle burned

r_{pm} = mass median particle diameter

t_{pm} = particle burning time of a mass median particle

σ = the standard deviation of the particle size distribution.

This equation is used as a tool for extrapolating existing data, since the constants required and the function H are not generally known.

6.3.4 Conclusions from Crowe's Theory

In conclusion, the main point of this analysis was that the major effect of the acceleration field was to move particles larger than the critical size to the propellant surface. The particles at the surface burn and release their energy at the propellant surface. The residence time of the particle at the surface was a function of the heat release rate, the particle size and the acceleration level. Further, it was predicted that when the mass median particle diameter was lower than the

critical diameter, the effects of acceleration will be small. In addition, if there are no metal oxide particles, there will be no effect regardless of acceleration level.

6.4 Conclusions

The two theories reviewed here are attempts to get at the most important factors influencing the burning rate augmentation in an acceleration environment. Glick's theory is primarily for nonalumized propellants and consists of a scalor and a vector effect. The scalar contribution was due to the increased relative motion between the fuel rockets and oxidizer vapor. The vector effect was associated with the compression or expansion of the gas phase reaction zone. The theory of Crowe et al. was based entirely upon metalized propellants and the effect of retaining larger metal particles upon the propellant surface. A further description of the validity of these theories in comparison to experimental results is given in a theses by Anderson (63) and Northam (64) which are reviewed with many other in reference (69).

7. SURVEY ARTICLES

7.1 Swithenbank and Sotter

In 1964 Swithenbank and Sotter (65, 66) presented an analysis of the effect of vorticies generated by combustion pressure oscillations on the performance of solid propellant rocket motors. The authors investigated the theories of vortex flow to determine their applicability in the chamber of a rocket motor, and they also investigated Mager's (3) analysis for rotating nozzle flows.

Applying incompressible viscous flow theory in the chamber, an estimate was made of the viscous effects upon the vortex distribution. For a typical six inch diameter rocket motor, the turbulent Reynolds numbers for the radial and tangential velocities were estimated. Based upon the turbulent velocity correlation of Keyes (67), these Reynold's number were estimated to be

$$R_{e,t} = 2 \times 10^5 \qquad R_{e,r} = 8.0 \tag{7.1}$$

Thus, it was concluded that the vortex motion will not appreciably be affected by viscous forces except possibly near the centerline. Employing the incompressible flow theory of Einstein and Li (15), it was found that the flow will be predominately free vortex in character except near the centerline where a solid body vortex should exist.

For the nozzle flow, viscous incompressible flow theory was discarded in favor of the inviscid compressible flow analysis of Mager (3). That

theory predicted a decrease in the mass flow and thrust producing capabilities of a nozzle due to the following factors:

1. A vacuum core, region on the centerline, and
2. A reduction in the mass flux at the throat.

For the measurements of the vorticies generated in their experimental studies, Swithenbank and Sotter found the mass flow to be reduced 70% when Mager's theory is applied. In addition to predicting the reduction of effective throat area, Mager's theory was used to predict observed irregular burning caused by vortex flow. A decrease in effective throat area can be related to the chamber pressure in the following manner.

$$A_b \dot{r} \rho_p = A_n^{**} P_c \nu \qquad (7.2)$$

where,

A_v = area of the burning surface

$\dot{r} = P^n$ = the burning rate

ρ_p = density of the propellant

A_n^{**} = the effective throat area

P_c = the chamber pressure

ν = characteristic velocity of the gases.

The following conclusions regarding the affects of rotation were made:

1. The decrease in effective throat area increased the chamber pressure.
2. The burning rate was increased due to increased chamber pressure.
3. Erosive effects of the vortex further increased the burning rate.

7.2 Crowe

A final report by Crowe (62) released in 1966 presents an excellent study of the many theories discussed in this literature survey. In addition, an investigation was made of the dynamics of particle flow in vorticies. The experimental portion of this research program is reviewed in Refs. 69. Therefore, only the analytical investigation will be discussed here.

The analysis of the flow in a rocket motor was divided into the following sections:

1. Solution for the viscous vortex motion in the rocket chamber.
2. Distribution of the metal oxide particles in the rocket chamber.
3. Effect of rotation upon nozzle performance.

7.2.1 Solution for the Viscous Vortex Motion in the Rocket Chamber

The analysis of the viscous vortex in the chamber was prefeced by a solution for the inviscid, compressible flow case. The inviscid compressible flow case was used as a comparison to estimate the effects of compressibility. The Euler equations are presented and solved in general terms under the conditions of conservation of angular momentum, assuming that all gas particles possess the same angular momentum since they originate at the same radial position.

$$u \frac{\partial(vr)}{\partial r} + w \frac{\partial(vr)}{\partial z} = \frac{d}{dt}(vr) = 0 \qquad (7.3)$$

$$v = \left(\frac{v_w r_w}{r}\right)$$

v_w = tangential velocity at the propellants surface

r_w = radius of the propellant surface

Since the motion of the vortex is irrotational and the flow is inviscid and adiabadic, the flow properties are governed by an isentropic expansion from the initial conditions.

The maximum velocity occurs when the static temperature becomes zero.

$$q_{max} = \sqrt{\left(\frac{2}{\gamma-1}\right)\gamma R T_o} \tag{7.5}$$

When the flow is viscous in nature, the shear stress will alter the free vortex solution. The shear stresses in the tangential direction are given by

$$\tau = \mu \left(\frac{\partial v}{\partial r} - \frac{v}{r}\right) = -2\mu \frac{v_w r_w}{r^2} \quad . \tag{7.6}$$

Thus as the radius decreases, the shear stresses increase.

$$\tau \propto (1/r)^2 \quad . \tag{7.7}$$

The viscous torque per unit length parallel to the flow becomes

$$M = + (2\pi r)\tau \cdot r = -4\pi\mu \; v_w r_w \quad . \tag{7.8}$$

Thus, the potential vortex gives a constant torque distribution. Because there existed a free boundary near the centerline, the torque at that point must vanish. Therefore, a solid body vortex should have existed near the centerline.

The approach to the viscous flow solution was that given by Burgers (11). In that case, the axial velocity was of the form

$$w = -2 u_w z/r_w \tag{7.9}$$

From the continuity equation

$$u = (r/r_w)\, u_w \,. \tag{7.10}$$

This procedure represents the stagnation vortex approach. Following the method of Burgers (11) and Rott (13, 14), which is a special case of the Donaldson and Sullivan solutions (16, 17, 18, 22), the tangential velocity was given by

$$\frac{v}{v_w} = \frac{1}{\eta}\left(\frac{1 - e^{-Re/4\ \eta^2}}{1 - e^{-Re/4}}\right) \tag{7.11}$$

where

$$\eta = r/r_w$$

$$Re = \frac{u_w\ 2\ r_w}{\nu} \,.$$

Pressure variations for the incompressible, viscous, vortex flow field in the chamber are obtained by employing Rott's analysis (13, 14), which is an extension to Burger's solution (13, 14).

$$P = P_c + \rho\, \frac{u_w^2}{2}\left[1 - \eta^2 - 4\left(\frac{z}{r_w}\right)^2\right] - \int_{\eta}^{1} \frac{v^2}{\eta}\, d\eta \tag{7.12}$$

where

P_c = pressure at the wall and head end of the grain.

The term on the right hand side involving the integral may be evaluated employing the expression derived earlier for the tangential velocity.

$$P = P_c + \rho \frac{uw^2}{2} [1 - n^2 - 4 (\frac{z}{r_w})^2] \frac{\rho\, Vw^2}{(1-e^{-Re/4})^2} (\frac{Re}{8}) f(\frac{\sqrt{Re}}{2}, n)$$

$$f(y) = \frac{e^{-Re/4}}{Re/4} \frac{(2-e^{-Re/4}}{} \frac{-e^{-y^2}}{y^2} [2 - e^{-y^2}] + \frac{1}{y^2} - \frac{4}{Re} \qquad (7.13)$$

$$+ [Ei (y^2) - Ei (\frac{Re}{H})] - [Ei (2y^2) - Ei (Re/2)]$$

where

$$Ei(x) = \int_{\alpha}^{\infty} \frac{e^{-t}}{t} dt, \qquad y = \frac{\sqrt{Re}}{2} n . \qquad (7.14)$$

In conclusion, the tangential velocity and the pressure functions were plotted for various values of Reynolds numbers from 1 to 10^6.

The higher the Reynolds number, the more the flow approaches a free vortex. For Reynolds numbers of the order of one, the entire flow field becomes forced vortex in character. Typical values of Reynolds number were postulated to be from 10^4 to 10^6, thus predicting that the tangential velocity was primarily free vortex in character, while the pressure gradient no longer increases with Reynolds number, as illustrated in Figures 14 and 15.

It should be noted that the Reynolds number was based upon the radial velocity at the propellant surface. The radial velocity was usually in the order of a few feet per second. In addition, the effects of turbulence are to increase the effective viscosity so that values of the radial Reynolds number are in the order of 10 (65, 67). Thus in an actual flow, the solid body core may be a considerable portion of the total flow.

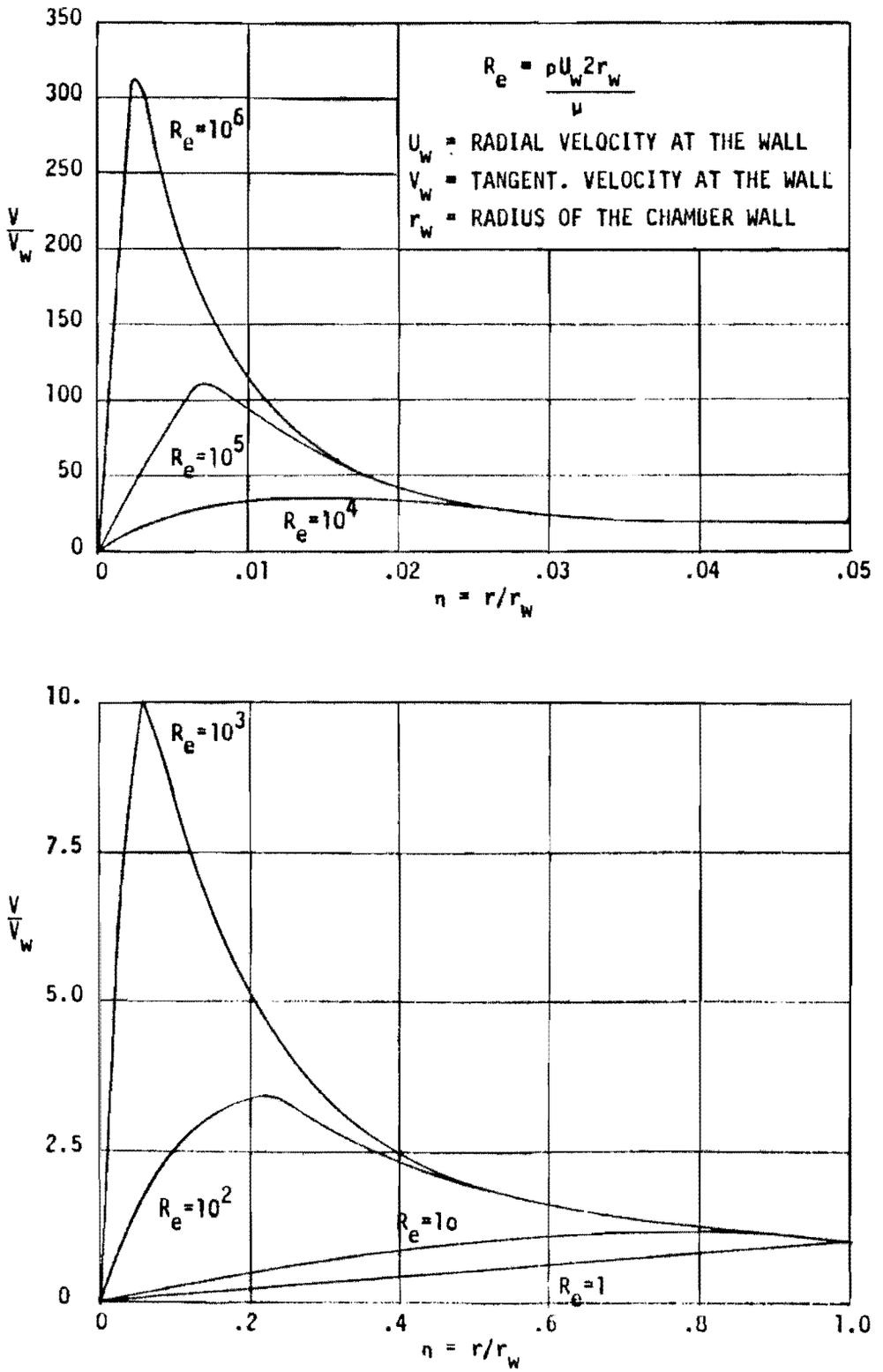

FIGURE 14 THE TANGENTIAL VELOCITY DISTRIBUTIONS AS A FUNCTION OF REYNOLD'S NUMBER USING BURGERS SOLUTION APPLIED TO INTERNAL BURNING MOTORS (62).
(Taken from reference (62) , Crowe et al.)

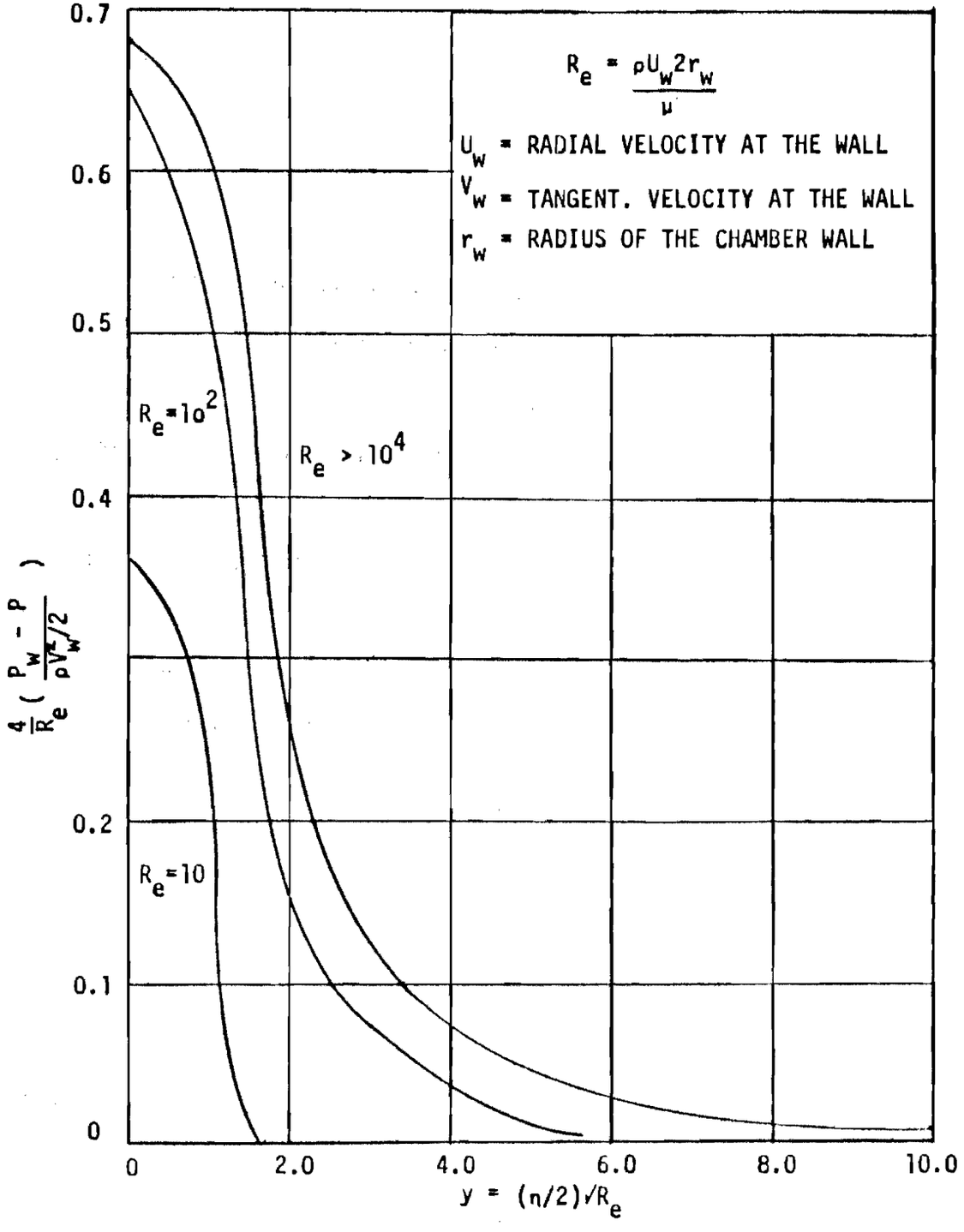

FIGURE 15 THE RADIAL PRESSURE DISTRIBUTION IN A CHAMBER OF AN INTERNAL BURNING MOTOR (62).
(Taken from reference (62) , Crowe et al.)

7.2.2 Distribution of the Metal Oxide Particle in the Rocket Chamber

The treatment of the metal oxide particles in the chamber was based upon the following assumptions:

1. The gas properties are independent of the particle properties and are those determined from a viscous, incompressible flow analysis.
2. The particles are in angular momentum equilibrium with the gasses.
3. The particles do not penetrate the viscous portion of the flow.
4. Stokes flow is assumed for the particles.

The following equations of motion for the particles were derived.

$$\frac{du}{dt} - \frac{u^2}{nr_w} = \frac{1}{\tau}(u_6 wn - u) \tag{7.15}$$

$$n\frac{dv}{dt} + \frac{uv}{r_\omega} = \frac{1}{\tau}(\omega r_w - v_n) \tag{7.16}$$

$$\frac{d\omega}{dt} = -\frac{1}{\tau}\left[2\ ugw\left(\frac{z}{r_w}\right) + \omega\right] . \tag{7.17}$$

Solutions for these equations were obtained analytically, and the distribution of the metal oxide particles was found. The results were plotted for typical particle diameters.

A critical radius, n_c, was found below which the solid particles cannot penetrate due to the centrifugal forces. The critical radius was proportional to the particle size and the square root of the motor spin rate.

For particles of the order of one micron, the maldistribution of particle mass flux was small for a spin rate of 1000 rpm or less, but could become appreciable for speeds greater than 10,000 rpm.

7.2.3 Effects of Rotation on Nozzle Performance

The analysis of the nozzle flow condition was based primarily upon Mager's analysis (3) of irrotational vorticies in rocket nozzles. Therefore, the rotational core predicted for viscous incompressible flow was neglected by assuming that it has a small area. Since the particles in the flow do not pass into the viscous region, the particle distribution can be found.

Since the particle distribution was determined at the nozzle inlet, it was only necessary to apply the radial momentum equation for the particles to determine their redistribution in the nozzle. The change in radial position is due to change in the centrifugal forces acting upon the particles, under the assumption of angular momentum equilibrium. Thus

$$\frac{dv_p}{dt} = \frac{V_w^2}{r^3} r_c^2 + \frac{3}{16} \mu \frac{C_D \, Re}{\rho_p \, \nu_p^2} (u_g - u_p) \qquad (7.18)$$

where, the first term on the right hand side is a centrifugal force term and the last term is the Stokes flow viscous term of the particle velocity lag in the radial direction.

In conclusion it was found that when,

R_t = 1.0 inches

P_c = 1000 psia

d_p = 1 micron

the effect of a rotating flow in a nozzle upon the particle flow is not large for spin rates below 6500 rpm. When the spin rate was larger, the effect on the particles increases. In addition, when the particle diameter was above 1 micron, the effect was accentuated so that an appreciable fraction of the particles are located at or near the wall.

8.0 SUMMARY

The field of contained rotating flows is rapidly growing and quite diverse. In this report only some of the possible areas of study have been examined. The primary emphasis has been placed upon the problem areas which would be found in rotating rocket motors. It is evident from the number and variety of the articles listed that a complete description of the flow in the nozzle and chamber of a rotating rocket motor is not yet possible. It should be noted that the analytical conveniences of infinite cylinders and rotating plates do not touch upon the interaction of the nozzle and the chamber flow fields.

In general the effect of rotation is to reduce the mass flux at the throat. This effect is accentuated by increasing the motor spin rate and by increasing the nozzle contraction ratio. However, a significant portion of this decrease may be negated by a transfer of angular momentum to the nozzle walls through viscous shear.

It appears possible that recirculating viscous flow patterns can be established from the action of the fore and aft end sections of the motor. Also, the boundary layer can transport significant portions of the mass from one area of the flow field to another. There is also a case for back flow patterns due to dynamic effects in the nozzle. These patterns, as predicted analytically, can be quite complex if the ratio of tangential to axial velocity becomes much greater than unity. Portions of these patterns tend, however, to be unstable to distrubances.

The effect of the reduction in mass flow rate at the throat is felt by the chamber as an effective decrease in throat area. This can cause increases in chamber pressure over the non-rotating condition. This increase in chamber pressure can be quite severe if the sensitivity of the propellant to pressure is large. The effect of backflow and recirculatory patterns is to produce variations in the local burning rates where these hot combustion gases tend to impinge upon the propellant.

In the chamber the effect of rotating flow is to set up pressure gradients which may alter the local burning rates. In addition, the acceleration forces accompanying the pressure gradients can cause retention of solid phases at the propellant surfaces or otherwise affect the combustion zone of the propellant.

NOMENCLATURE

English Symbols

a = accoustic speed

a_o = stagnation accoustic speed

C = $V \circ r$ - angular momentum

c_p = specific heat at constant pressure

D = diameter

H = enthalpy

$\dot{m}$ = mass flow rate

n = burning rate index; tangential velocity exponent $v = k/r^n$.

P = pressure

Q = volume flow rate

q = the total velocity

R = gas constant

R_w = radius of the wall

Re = Reynolds number

r = radial space coordinate

S = entropy

T = temperature

u = radial velocity

v = tangential velocity

w = axial velocity

z = the axial space coordinate

Greek Symbols

Γ = angular momentum

γ = specific heat ratio

δ, Δ = boundary layer thicknesses

ε = eddy viscosity

ζ = z/ℓ reduced axial coordinate

η = $(r/r_o)^2$ reduced radial coordinate

θ = the tangential coordinate; flow angle

μ = absolute viscosity

ν = μ/ρ, kinematic viscosity

π = 3.14159

ρ = density

σ = flow ratio - $u\ r\ \rho/\mu$

τ = shear stress

ϕ = velocity potential function

ψ = stream function

ω = angular velocity

$\bar{\omega}$ = vorticity vector

Subscripts

1 = initial condition

o = stagnation condition; total

p = particle

τ = tangential; total

w = wall

eff = effective

* = reduced condition, throat condition

LIST OF REFERENCES

1. Binnie, A. M. and Hooker, S. G., "The Radial and Spiral Flow of a Compressible Fluid," Proc. Royal Soc., Vol. A 159, 597-606 (1937)

2. Binnie, A. M., "The Passage of a Perfect Fluid Through a Critical Cross Section or 'Throat'," Proc. Royal So., Vol A 197 545-555, (1949)

3. Mager, A., "Approximate Solution of Isentropic Swirling Flow Through a Nozzle," ARS, Vol. 31, No. 8. 1140-1148 (Aug 1961)

4. Shapiro, A. H., The Dynamics and Thermodynamics of Compressible Fluid Flow, Vol I, New York, The Ronald Press Co., 1953, 280-282.

5. Vaszonyi, A., "On Rotational Gas Flows," Quart: Appl. Math., Vol 3, No. 1, 29-37 (1945)

6. Owczarck, J. A., Fundamentals of Gas Dynamics, Scranton Pa., Int. Text Book Co., 1964, 77-89.

7. Bastress, E. Karl, "Interior Ballistics of Spinning Solid-Propellant Rockets", AIAA Journal of Spacecraft, Vol 2, 455-457, (May-June 1965)

8. Manda, L. J. "Spin Effects on Rocket Nozzle Performance," Vol 3, No. 11, 1695-1606, (Nov. 1966)

9. King, M. K., "Commenton Spin Effects on Rocket Nozzle Performance," Vol 3, No 12, 1812-1813, (Dec. 1966)

10. Hall, M. G., "The Structure of Concentrated Vortex Cores," Progress in Aeronautical Sciences, ed. Kuchemann, D., New York, Permagon Press, 53-110, (1966)

11. Burgers, J. M., Application of a Model System to Illustrate Some Points of Statistical Theory of Free Turbulence," Proc. Acad. Sc: Amsterdam, Vol 43, No. 1, 2-12, (1940)

12. Burgers, J. M., Advances in Applied Mechanics, "A Mathematical Model Illustrating the Theory of Turbulence," Academic Press, Vol 1, 197-199 (1948).

13. Rott, N., "On the Viscous Core of a Line Vortex," ZAMP, Vol 9b, No. 5-6, 543-553, (1958).

14. Rott, N., "On the Viscous Core of a Line Vortex II," ZAMP, Vol 10, No. 1, 73-81 (1959).

15. Einstein, H. A., Li, H., "Steady Vortex Flow of a Real Fluid," Proc. Heat Trans. and Fluid Mech. Inst., 33-43, (1951).

16. Donaldson, C. duPont, "Solutions of the Navier-Stakes equations for Two and Three-Dimensional Vortices," Princeton Dissertation, (1956).

17. Donaldson, C. duPont, Sullivan, R. D., "Behavior of Solutions of the Navier-Stokes Equations for a Class of Three-Dimensional Viscous Vortices," Proc. 1960 Heat Transfer and Fluid Mechanics Inst., Stanford University pp 16-30, (June 1960).

18. Donaldson, C. duPont, "Examination of the Solutions of the Navier-Stokes Equations for a Class of Three-Dimensional Vortices," ARAP Report, No. 51, (Nov. 1963).

19. Lay, J. E., "An Experimental and Analytical Study of Vortex Flow Temperature Separation by Superposition of Spiral and Axial Flow, Part 1," ASME J. of Heat Transfer, 202-212, (Aug. 1959).

20. Lay, J. E. "An Experimental and Analytical Study of Vortex Flow Temperature Separation by Superposition of Spiral and Axial Flow, Part 11," ASME J. of Heat Transfer, 213-223, (Aug. 1959).

21. Pengelly, C. D., "Flow in a Viscous Vortex," J. Appl. Phys., Vol. 28, No. 1, 86-96, (Jan. 1957).

22. Deissler, R. G., and Perlmutter, Morris, "An Analysis of the Energy Separation in Laminar and Turbulent Compressible Vortex Flows," Proc. Heat Transfer and Fluid Mech. Inst., 1958.

23. Sullivan, R. D., A Two-Cell Vortex Solution of the Navier-Stokes Equations," J. of Aerospace Sci., 767-768, (Nov. 1959).

24. Sibulkin, M., "Unsteady, Viscous, Circular Flow - Part I - The Line Impulse of Angular Momentum," J. of Fluid Mech., Vol II, 291-308 (1961).

25. Sibulkin, M., "Unsteady, Viscous, Circular Flow - Part 2 - The Cylinder of Finite Radius," J. of Fluid Mech., Vol. 12, 148-148 (1961).

26. Sibulkin, M., "Unsteady, Viscous, Circular Flow - Part 3 - Application to the Ranque - Hilsch Vortex Tube," J. of Fluid Mech., Vol 12, Part 2, 269-293, (Feb. 1962).

27. Lewellen, W. S., "A Solution for Three-Dimensional Vortex Flows with Strong Circulation," J. of Fluid Mech., Vol 14, Part 3, 420-432, (1962).

28. Lewellen, William S., 1964, "Three Dimensional Viscous Vortices in Incompressible Flow," Thesis, Univ. of California, Los Angeles, (1964).

29. Lewellen, W. S., "Linearized Vortex Flow", AIAA Journal, Vol. 3, No. 1, 91-98, (Jan 1965).

30. Taylor, G. I., "The Mechanics of Swirl Atomizers," 7th Int. Congress for App. Mech., Vol. 2, 280-285, (1940).

31. Taylor, G. I., The Boundary layer in the Converging Nozzle of a Swirl Atomizer," Quart. J. of Mech. and Appl. Math., Vol 3, Part 2, 129-139 (1950).

32. Binnie, A. M., Harris, D. P., "The Application of Boundary-layer Theory to Swirling Liquid Flow Through a Nozzle," Quart. J. Mech. and Appl. Math., Vol 3, Part 1, 89-106, (1950).

33. Cooke, J. C., "On Pohlhausen's Method with Application to a Swirl Problem of Taylor's", Journal of Aeronautical Sciences, 486-490, July 1952.

34. Weber, H. E., "The Boundary Layer Inside a Conical Surface Due to Swirl", Journal of Applied Mechanics, 587-592, (Dec. 1956).

35. Schlichting, H., Boundary Layer Theory, 4th Edition, McGraw-Hill Co., New York, 176-181, (1960).

36. Batchelor, G. K., "Note on a Class of Solutions of the Navier-Stokes Equations Representing Steady Rotationally-Symmetric Flow," Quart. J. Mech. and Appl. Math., Vol 4, Part 1, (1951).

37. Rogers, M. H. and Lance, G. N., "The Rotationally Symmetric Flow of a Viscous Fluid in the Presence of an Infinite Rotating Disk," Journal of Fluid Mech., Vol. 7, 617- , (1960).

38. Mack, L. M., "The Laminar Boundary Layer on a Disk of Finite Radius in Rotating Flow - Part I," J.P.L. Tech. Report., No. 32-224 (May 1962).

39. Mack, L. M., "The Laminar Boundary Layer on a Disk of Finite Radius in Rotating Flow - Part II," J.P.L. Tech. Report No. 32-366, (Jan 1963).

40. Lewellen, W. S., King, W. S., "The Boundary Layer of a Conducting Vortex Flow Over a Disk with an Axial Magnetic Field," Aerospace Tech. Note ATN-63(9227)-1, (Dec. 1962).

41. King, W. S., "Momentum-Integral Solutions for the Laminar Boundary Layer on a Finite Disk in a Rotating Flow," Aerospace Tech. Report ATN-63(9227)-3 (June 1963).

42. King, W. S., Lewellen, W. S.,"Boundary-Layer Solutions for Rotating Flows with and Without Magnetic Interaction," Aerospace Tech. Report. No. ATN-63(9227)-6 (July 1963).

43. Rosenzweig, M. L., Lewellen, W. S., Ross, D. H., "Confined Vortex Flows with Boundary-Layer Interaction," AIAA Journal, Vol. 2, No. 12, 2127-2134, (Dec. 1964).

44. Rott, N., Lewellen, W. S., Boundary Layers in Rotating Flows, Aerospace Corp., ATN-64(9227)-6, El Segundo,Calif. (Sept. 1964).

45. Rott, N., Lewellen, W. S., Progress in Aeronautical Sciences - Vol 7, "Boundary Layers and Their Interactions in Rotating Flows," ed. Kuchenman, D., New York Rermagon Press, 111-144, (1966).

46. Rayleigh, J. W. S., "On the Stability or Instability of Certain Fluid Motions," Proc. London Math. Soc., 11, 57-70 (1880), also, Scientific Papers, Vol I, 474-487.

47. Rayleigh, J. W. S., "On the Stability of Certain Fluid Motions, II.," Proc. London Math. Soc., 19, 67-74, (1887), also, Scientific Papers Vol III, 17-23.

48. Rayleigh, J. W. S., "On the Question of Stability of the Flow of Fluids," Phil. Mag. 34, 59-70 (1892), also, Scientific Papers, Vol III, 575-584.

49. Kelvin, Lord, Mathematical and Physical Papers, Vol 4, Hydrodynamics and General Dynamics, Cambridge, University Press, (1960).

50. Ludweig, H., "Zur Erklarung der Instabilitat der Angestellen Deliaflugeln Auftretenden Frein Wirkbelkerne," Z. Flugw. 10, 242-249, (1962).

51. Keissling, I., "Uber das Taylorskhe Stabilitats-problem bet Zuzatzlicher axialer Durch stromung der Zylinder, DVL Bench Nr. 2963, (1963).

52. Weske, J. R., "The Effect of Stretching of a Vortex Core," Univ. of Maryland Tech. Note BN-57, (Aug. 1955).

53. Burgers, J. M., "The Effect of Stretching of a Vortex Core," Univ. of Maryland Tech. Note BN-80, (Aug. 1956).

54. Squire, H. B., "Analysis of the Vortex Breakdown Phenomenon, Part I, Aero. Dept., Imperial Coll., Rep. No. 102, (1960).

55. Benjamin, T. Brooke, "Theory of the Vortex Breakdown Phenomenon," J. of Fluid Mech., Vol 14, Part 4, 593-629, (Dec. 1962).

56. Harvey, J. K., "Some Observations of the Vortex Breakdown Phenomenon," J. of Fluid Mech., Vol. 14, Part 4, 585-592, (Dec. 1962).

57. Benjamin, T. Brooke, "Significance of the Vortex Breakdown Phenomenon," ASME Paper No., WA/FE-18, 1964.

58. Lambourne, N. C., "The Breakdown of Certain Types of Vortex," National Physical Laboratory, Aerodynamics Division, NPL Aero Report 1166, (September 1965).

59. Gore, R. W., Ranz, W. E., "Backflows in Rotating Fluids Moving Axially Through Expanding Cross Sections," A.I. Ch. E. J., Vol 10, 83- (Jan 1964).

60. Glick, R. L., "The Effect of Acceleration on the Burning Rate of Non-metallized Composite Propellants," Ph.D. Thesis, Purdue Univ. (Aug. 1966).

61. Summerfield, M. et al., "Burning Mechanisms of Ammonium Perchlorate Propellants," Progress in Astronautics and Rocketry, Academic Inc., New York, New York, 1960, Vol 1, 141-182.

62. Crowe, C. J., et al., "Investigation of Particle Growth and Ballistic Effects on Solid Propellant Rockets," U.T.C. Report VTC 2128-Fr, (June 1966).

63. Anderson, J. B., "An Investigation of the Effect of Acceleration on the Burning Rate of Composite Propellants," Ph.D. Thesis, U.S. Naval Post Graduate School, (Aug. 1966).

64. Northam, "An Experimental Investigation of the Effects of Acceleration on the Combustion Characteristics of an Alumized Composite Solid Propellant," M.S. Thesis, V.P.I, (June 1965).

65. Swithenbank, J., Sotter, G., "Vortex Generation in Solid Propellant Rockets," AIAA Preprint No. 64-144, (Jan. 1964).

66. Swithenbank, J., Sotter, G., "Vortices in Solid Propellant Rocket Motors," AIAA J. Tech. Note, Vol 1, No. 7, 1682-1685, (July 1964).

67. Keyes, J. J., "An Experimental Study of Flow and Separation in Vortex Tubes with Application to Gaseous Fusion Heating," ARS Preprint 1516-60 (1960).

68. Farquhar, B. W., Norton, D. J., Hoffman, J. D., "Investigation of High Acceleration on the Interior of Solid Propellant Rocket Motors," Jet Propulsion Center, Purdue University, Report No. F-66-10 (December 1966).

69. Farquhar, B. W., Norton, D. J., Hoffman, J. D., "Experimental Studies of the Interior Ballistics of Spinning Rocket Motors - A Literature Survey," Jet Propulsion Center, Purdue University, Report No. TM 67-2 (January 1967).